# Aeroelastic Prediction Workshop

## *Data Analysis*

Presented by:

Jennifer Heeg

Aeroelasticity Branch, NASA Langley Research Center

On behalf of the AePW Organizing Committee

# *Contents*

- Status of data analyses
- Comparison results:  Describe the data analysis processes for the experimental data sets
    - Steady data
    - Frequency response functions
- Displacement amplitude for input to analyses

# Comparison Data Matrix

| CONFIGURATION | REQUIRED CALCULATIONS | | | |
|---|---|---|---|---|
| | GRID CONVERGENCE STUDIES | TIME CONVERGENCE STUDIES | STEADY CALCULATIONS | DYNAMIC CALCULATIONS |
| Steady-Rigid Cases (RSW, BSCW) | $C_L$, $C_D$, $C_M$ vs. $N^{-2/3}$ | n/a | • Mean $C_p$ vs. x/c<br>• Means of $C_L$, $C_D$, $C_M$ | n/a |
| Steady-Aeroelastic Cases (HIRENASD) | $C_L$, $C_D$, $C_M$ vs. $N^{-2/3}$ | n/a | • Mean $C_p$ vs. x/c<br>• Means of $C_L$, $C_D$, $C_M$<br>• Vertical displacement vs. chord<br>• Twist angle vs. span | n/a |
| Forced Oscillation Cases (all configurations) | • Magnitude and Phase of CL, CD, CM vs. $N^{-2/3}$ at excitation frequency | • Magnitude and Phase of $C_L$, $C_D$, $C_M$ vs. $\Delta t$ at excitation frequency | n/a | • Magnitude and Phase of $C_p$ vs. x/c at span stations corresponding to transducer locations<br>• Magnitude and Phase of $C_L$, $C_D$, $C_M$ at excitation frequency<br>• Time histories of $C_p$'s at a selected span station for two upper- and two lower-surface transducer locations |

# Comparison Data Matrix: Experimental Data Analysis

Completed | In progress | Stalled

| CONFIGURATION | REQUIRED CALCULATIONS | | | |
|---|---|---|---|---|
| | GRID CONVERGENCE STUDIES | TIME CONVERGENCE STUDIES | STEADY CALCULATIONS | DYNAMIC CALCULATIONS |
| Steady-Rigid Cases (RSW, BSCW) | $C_L$, $C_D$, $C_M$ vs. $N^{-2/3}$ | n/a | • Mean $C_p$ vs. x/c<br>• Means of $C_L$, $C_D$, $C_M$ | n/a |
| Steady-Aeroelastic Cases (HIRENASD) | $C_L$, $C_D$, $C_M$ vs. $N^{-2/3}$ | n/a | • Mean $C_p$ vs. x/c<br>• Means of $C_L$, $C_D$, $C_M$<br>• Vertical displacement vs. chord<br>• Twist angle vs. span | n/a |
| Forced Oscillation Cases (all configurations) | • Magnitude and Phase of CL, CD, CM (vs. $N^{-2/3}$ at excitation frequency) | • Magnitude and Phase of $C_L$, $C_D$, $C_M$ (vs. $\Delta t$ at excitation frequency) | n/a | • Magnitude and Phase of $C_p$ vs. x/c at span stations corresponding to transducer locations<br>• Magnitude and Phase of $C_L$, $C_D$, $C_M$ at excitation frequency<br>• Time histories of $C_p$'s at a selected span station for two upper- and two lower-surface transducer locations |

# *In-progress Experimental Data Analysis: Balance loads*

**Balance data exists for calculating comparison data only for HIRENASD**

**Status:** Not complete

**Issues:** Axis definitions, orientation, normalizations, transformations, other?

From Aachen University published results

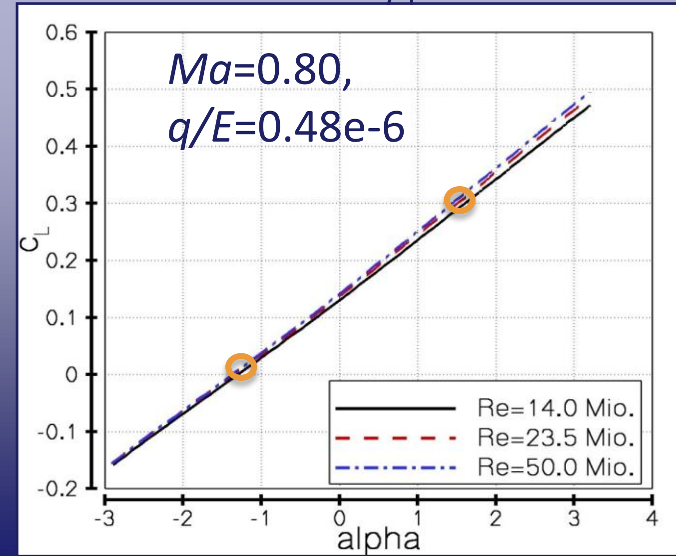


| CONFIGURATION | STUDIES | STUDIES | STEADY CALCU | |
|---|---|---|---|---|
| Steady-Rigid Cases (RSW, BSCW) | $C_L$, $C_D$, $C_M$ vs. $N^{-2/3}$ | n/a | • Mean $C_p$ vs. x<br>• Means of $C_L$, C | |
| Steady-Aeroelastic Cases (HIRENASD) | $C_L$, $C_D$, $C_M$ vs. $N^{-2/3}$ | n/a | • Mean $C_p$ vs. x/c<br>• Means of $C_L$, $C_D$, $C_M$<br>• Vertical displacement vs. chord<br>• Twist angle vs. span | n/a |
| Forced Oscillation Cases (all configurations) | • Magnitude and Phase of CL, CD, CM (vs. $N^{-2/3}$ at excitation frequency) | • Magnitude and Phase of $C_L$, $C_D$, $C_M$ (vs. $\Delta t$ at excitation frequency) | n/a | • Magnitude and Phase of $C_p$ vs. x/c at span stations corresponding to transducer locations<br>• Magnitude and Phase of $C_L$, $C_D$, $C_M$ at excitation frequency<br>• Time histories of $C_p$'s at a selected span station for two upper- and two lower-surface transducer locations |

# Steady (Static) Experimental Data

| CONFIGURATION | REQUIRED CALCULATIONS | | | |
|---|---|---|---|---|
| | GRID CONVERGENCE STUDIES | TIME CONVERGENCE STUDIES | STEADY CALCULATIONS | DYNAMIC CALCULATIONS |
| Steady-Rigid Cases (RSW, BSCW) | $C_L$, $C_D$, $C_M$ vs. $N^{-2/3}$ | n/a | • Mean $C_p$ vs. x/c<br>• Means of $C_L$, $C_D$, $C_M$ | n/a |
| Steady-Aeroelastic Cases (HIRENASD) | $C_L$, $C_D$, $C_M$ vs. $N^{-2/3}$ | n/a | • Mean $C_p$ vs. x/c<br>• Means of $C_L$, $C_D$, $C_M$<br>• Vertical displacement vs. chord<br>• Twist angle vs. span | n/a |
| Forced Oscillation Cases (all configurations) | • Magnitude and Phase of CL, CD, CM vs. $N^{-2/3}$ at excitation frequency | • Magnitude and Phase of $C_L$, $C_D$, $C_M$ vs. $\Delta t$ at excitation frequency | n/a | • Magnitude and Phase of $C_p$ vs. x/c at span stations corresponding to transducer locations<br>• Magnitude and Phase of $C_L$, $C_D$, $C_M$ at excitation frequency<br>• Time histories of $C_p$'s at a selected span station for two upper- and two lower-surface transducer locations |

# *Steady (or Static) Pressure Coefficients*

- RSW:
  - Historical tabulated values, obtained from archival publications, available through RTO
  - Based on steady state measurements; mean values
- BSCW
  - Calculated from time history data
  - Steady point: Mixed mean and mode values
  - Oscillatory points: Mean values of unsteady time histories
- HIRENASD
  - Angle of attack polar data:  pressures did not stabilize
  - Non-excitation portions of oscillatory time histories used; mean values

# BSCW Steady Pressure Distribution

- Non-oscillatory data point:
  - For almost all sensors:
    - Mean value calculated
    - +/- 3 standard deviations used as upper and lower bounds
  - For shock-traversed sensor:
    - Mode value calculated
    - 1% and 99% values used as upper and lower bounds
- Oscillatory data point:
  - Mean values calculated

# BSCW steady data

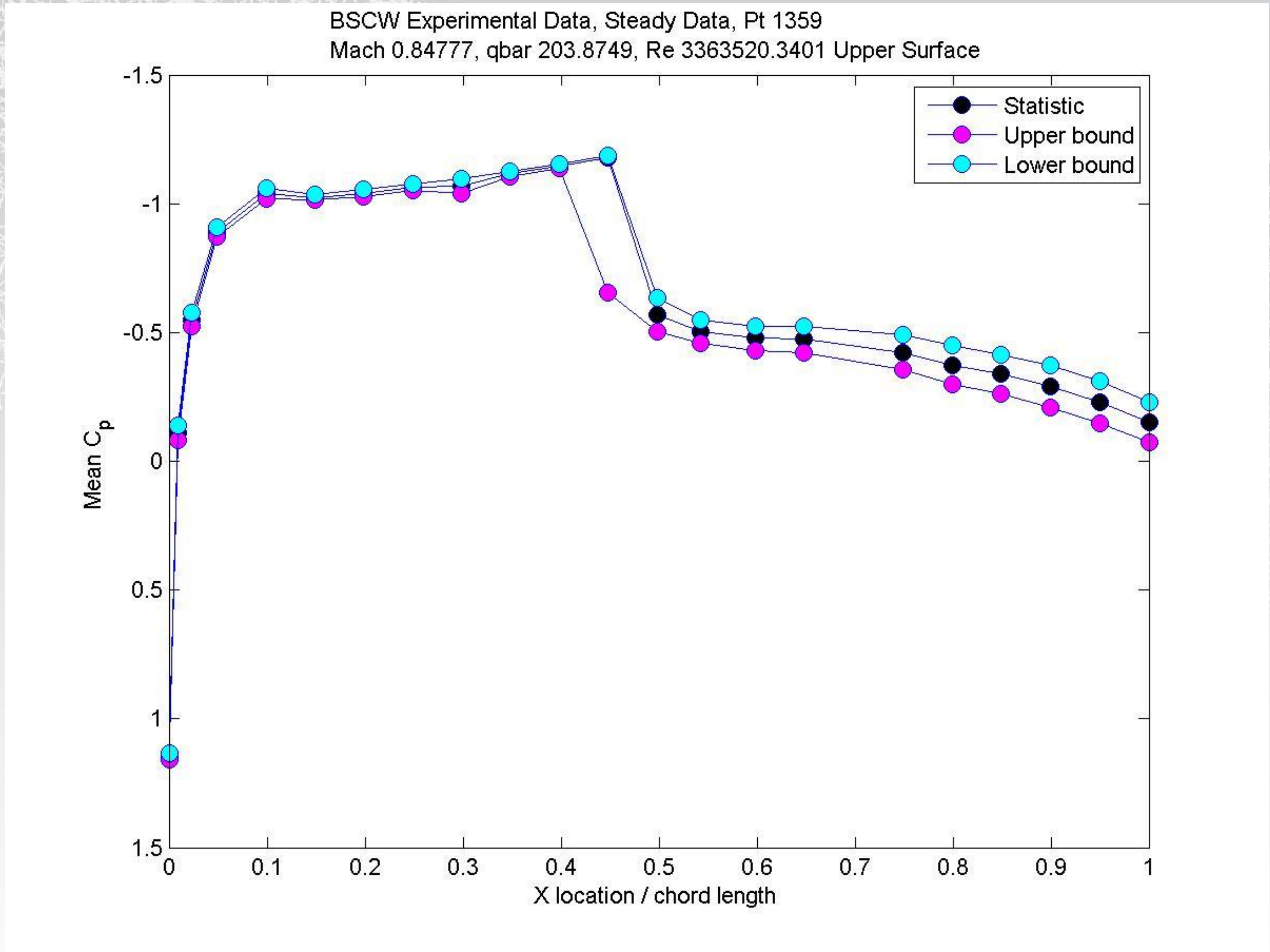

# BSCW Static Data:
# Steady Cp estimates from non-oscillated data

Data is assumed to be Gaussian when the mean is calculated.
For BSCW:
Most pressures are approximately Gaussian
Data in the region of the shock is poorly represented in this way

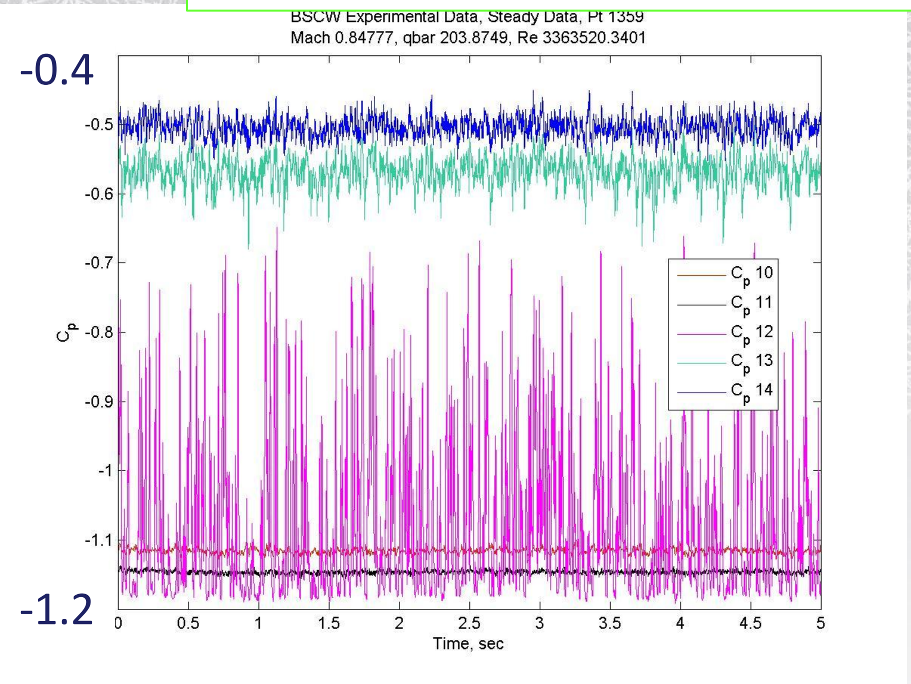


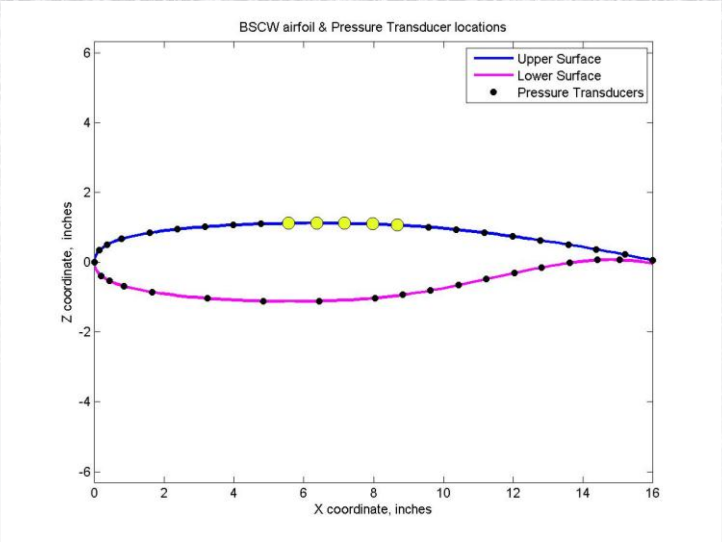


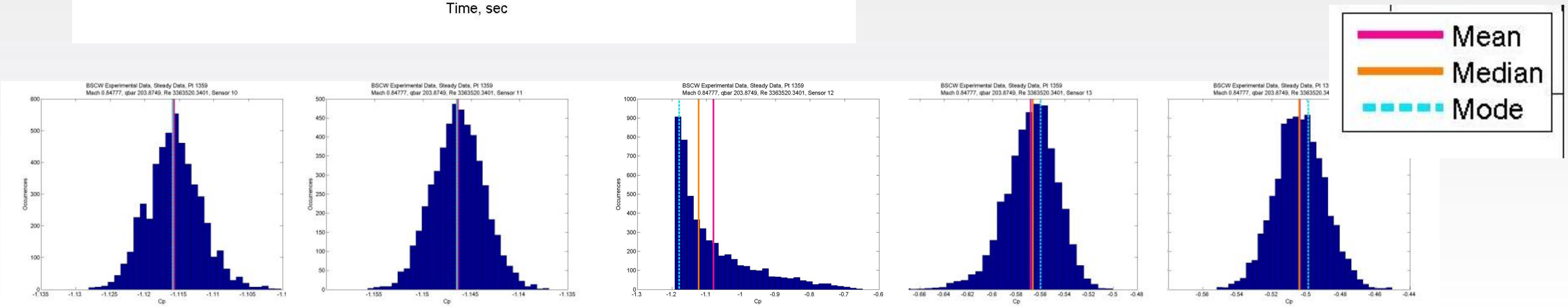

# BSCW Static Data:
# Steady Cp estimates from non-oscillated data

Using the mean value to represent the steady distribution:
Shock strength underestimated

- → Value at transducer 12: Mean value is 8% too low if mode is considered as the proper estimated value
- → The lower bound shown, turquoise circle, represents a value that is never achieved (overestimate of bound)
- → The upper bound, magenta circle, does not capture 99% of the data which is implied by the 3$\sigma$ calculations (underestimate of bound)
- → Mode, 99% and 1% values used instead of mean and std for this point

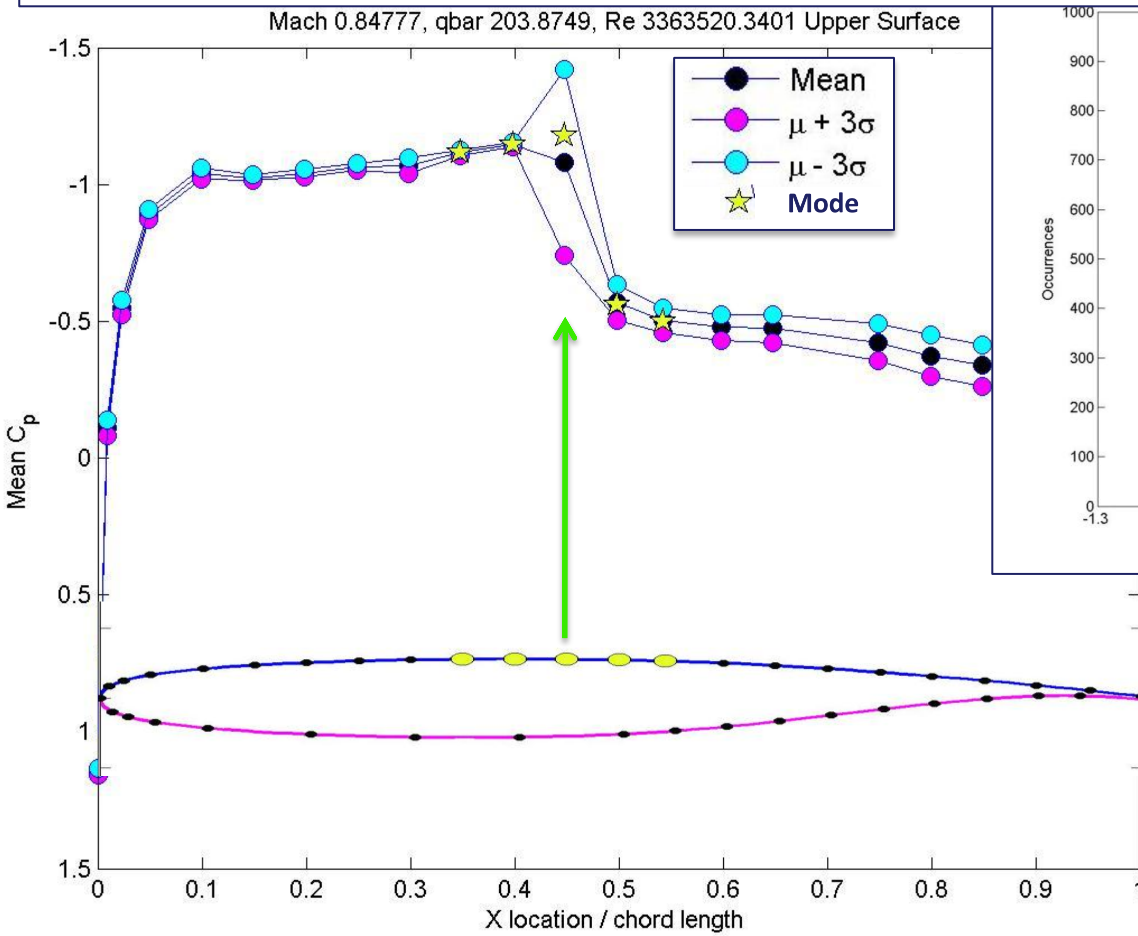


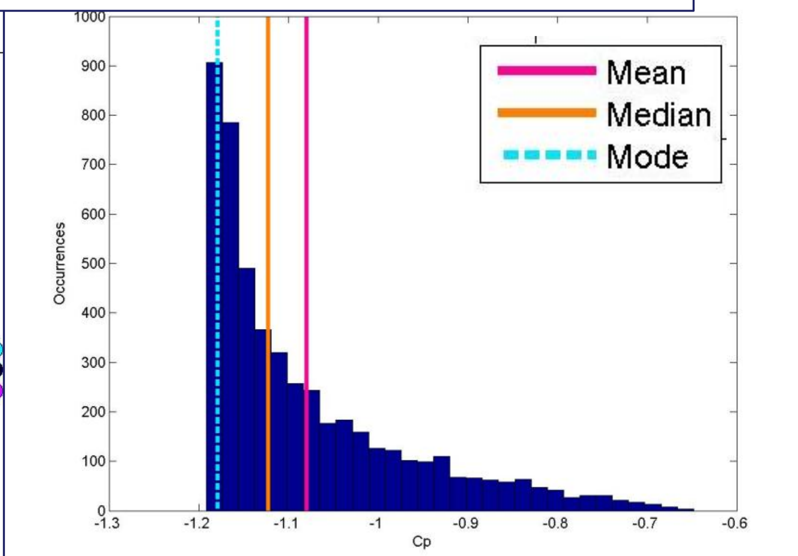

# BSCW Static Point, Lower Surface

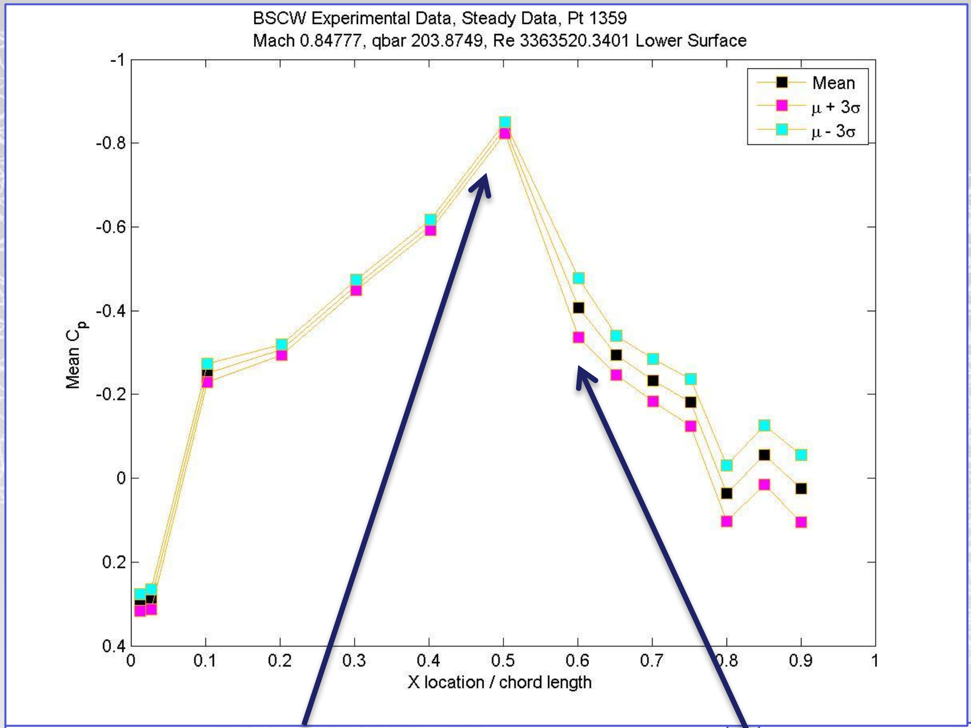


- Sensor 32 was not functional
- While variations for sensors aft of lower surface shock (?) is larger, the distributions are relatively Gaussian
- Mean and Std used to represent all lower surface points

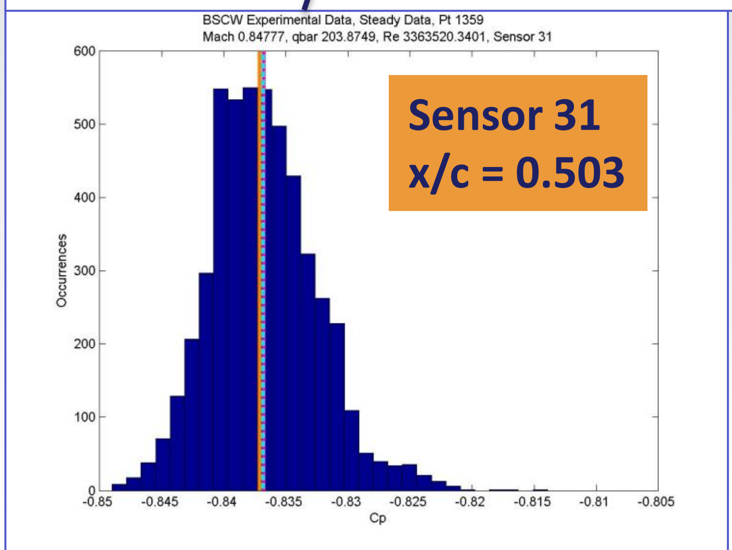


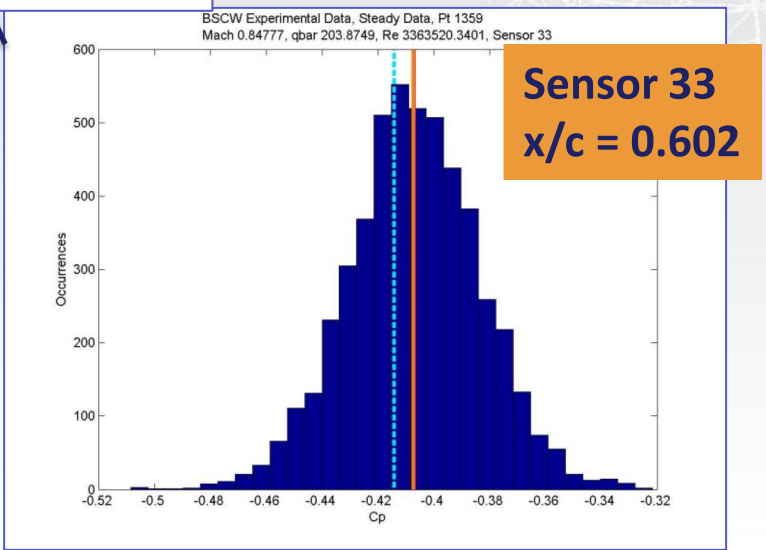

# *HIRENASD Static Data*

- Mode not used as replacement for HIRENASD data
  - It's more difficult
    - More sensors to evaluate
    - More cases to evaluate
  - Gaussian assumption not as bad as for BSCW shock
  - Multiple sensors display "moderately" non-Gaussian characteristics
  - Need method to quantify "good enough" in terms of Gaussian assumption
  - OR … Decide to replace mean and standard deviation with other statistics

# *HIRENASD Steady Data Selection*

- Each HIRENASD oscillatory point contains 2 regions of oscillation:  low excitation and high excitation
- These excitations are separated by several seconds

# *HIRENASD data subset for static analysis: time histories*

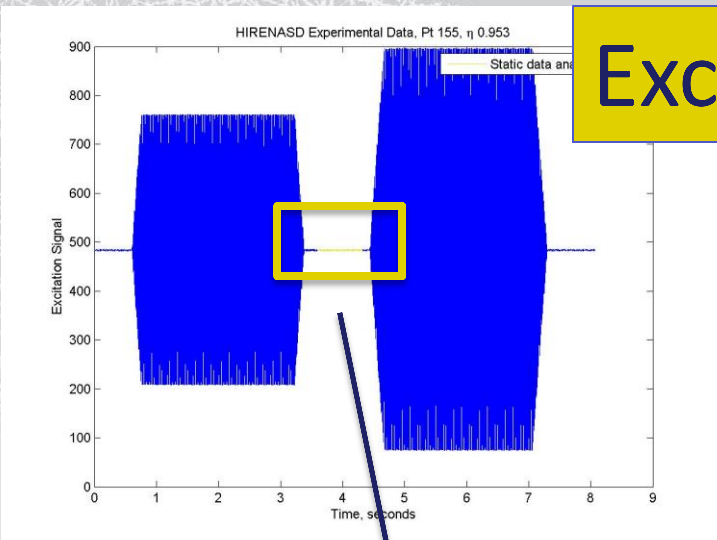


Excitation signal

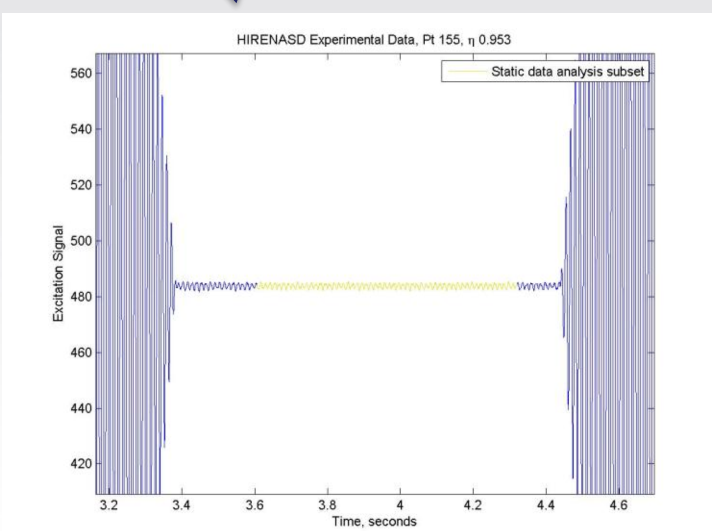


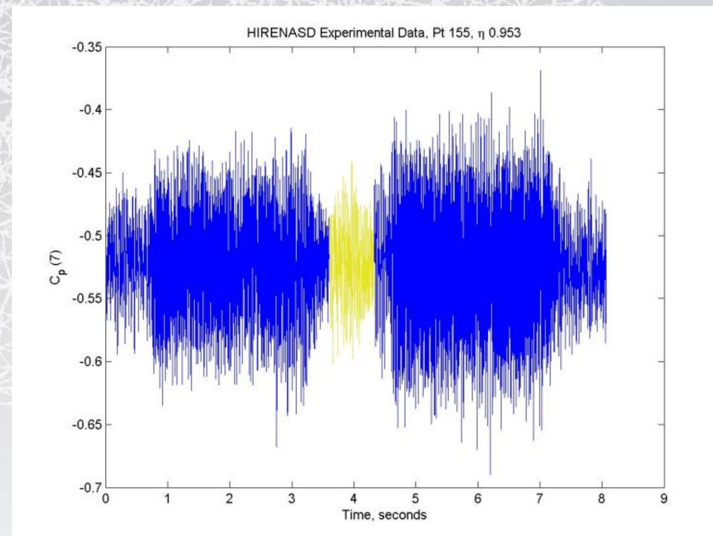


Example pressure subset

# Frequency Response Functions

| CONFIGURATION | REQUIRED CALCULATIONS | | | |
|---|---|---|---|---|
| | GRID CONVERGENCE STUDIES | TIME CONVERGENCE STUDIES | STEADY CALCULATIONS | DYNAMIC CALCULATIONS |
| Steady-Rigid Cases (RSW, BSCW) | $C_L$, $C_D$, $C_M$ vs. $N^{-2/3}$ ✓ | n/a | • Mean $C_p$ vs. x/c ✓<br>• Means of $C_L$, $C_D$, $C_M$ ✓ | n/a |
| Steady-Aeroelastic Cases (HIRENASD) | $C_L$, $C_D$, $C_M$ vs. $N^{-2/3}$ ✓ | n/a | • Mean $C_p$ vs. x/c ✓<br>• Means of $C_L$, $C_D$, $C_M$ ✓<br>• Vertical displacement vs. chord ✓<br>• Twist angle vs. span ✓ | n/a |
| Forced Oscillation Cases (all configurations) | • Magnitude and Phase of $C_L$, $C_D$, $C_M$ vs. $N^{-2/3}$ at excitation frequency ✓ | • Magnitude and Phase of $C_L$, $C_D$, $C_M$ vs. $\Delta t$ at excitation frequency ✓ | n/a | • Magnitude and Phase of $C_p$ vs. x/c at span stations corresponding to transducer locations<br>• Magnitude and Phase of $C_L$, $C_D$, $C_M$ at excitation frequency<br>• Time histories of $C_p$'s at a selected span station for two upper- and two lower-surface transducer locations |

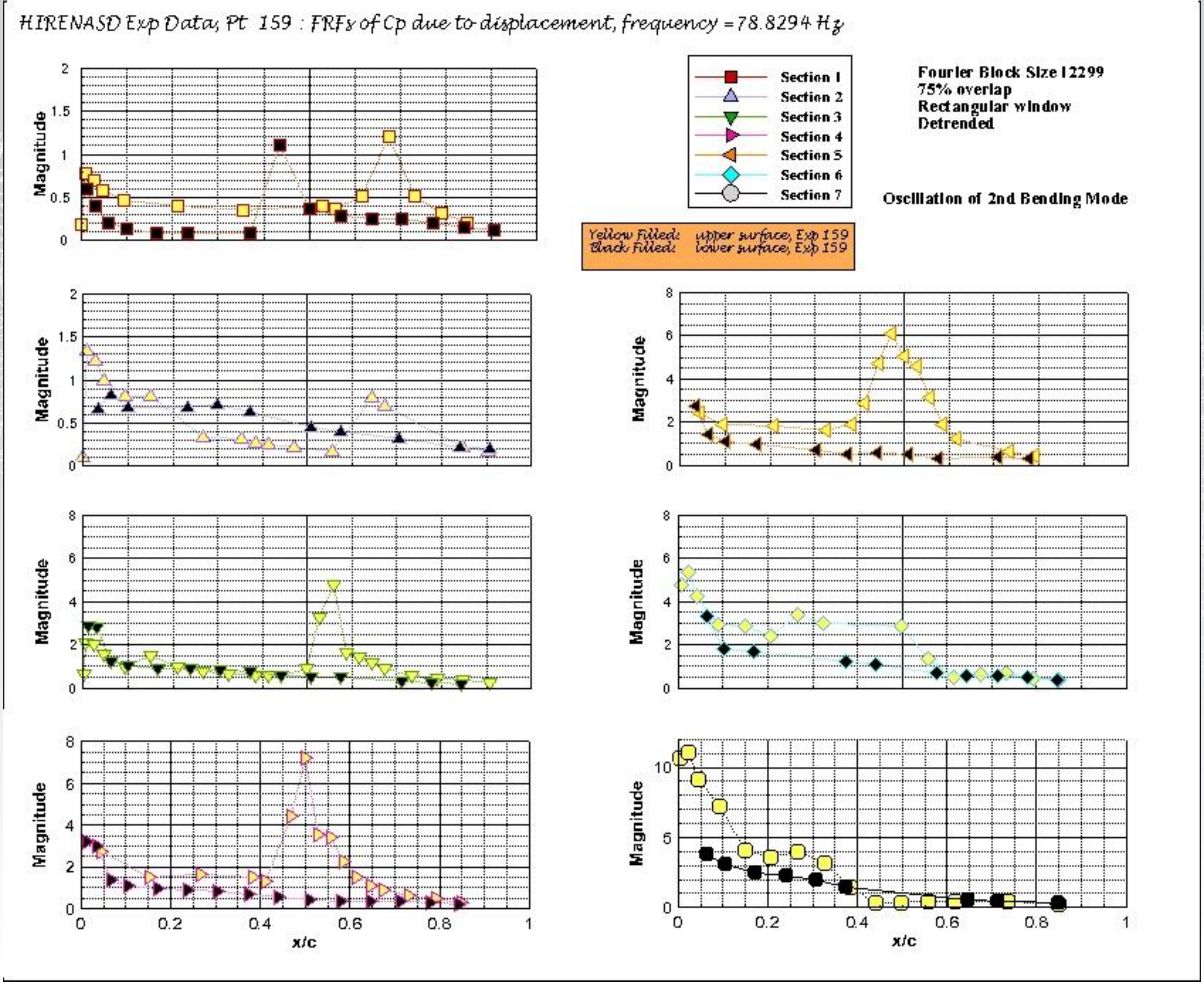
HIRENASD Exp Data, Pt 159 : FRFs of Cp due to displacement, frequency = 78.8294 Hz
Section 1
Section 2
Section 3
Section 4
Section 5
Section 6
Section 7
Fourier Block Size 12299
75% overlap
Rectangular window
Detrended
Oscillation of 2nd Bending Mode
Yellow Filled: upper surface, Exp 159
Black Filled: lower surface, Exp 159
Magnitude
x/c

# *Considerations in computing FRFs*

- Subset selection
- Displacement by integration of acceleration
- Fourier analysis block size determination

# *HIRENASD oscillatory data*

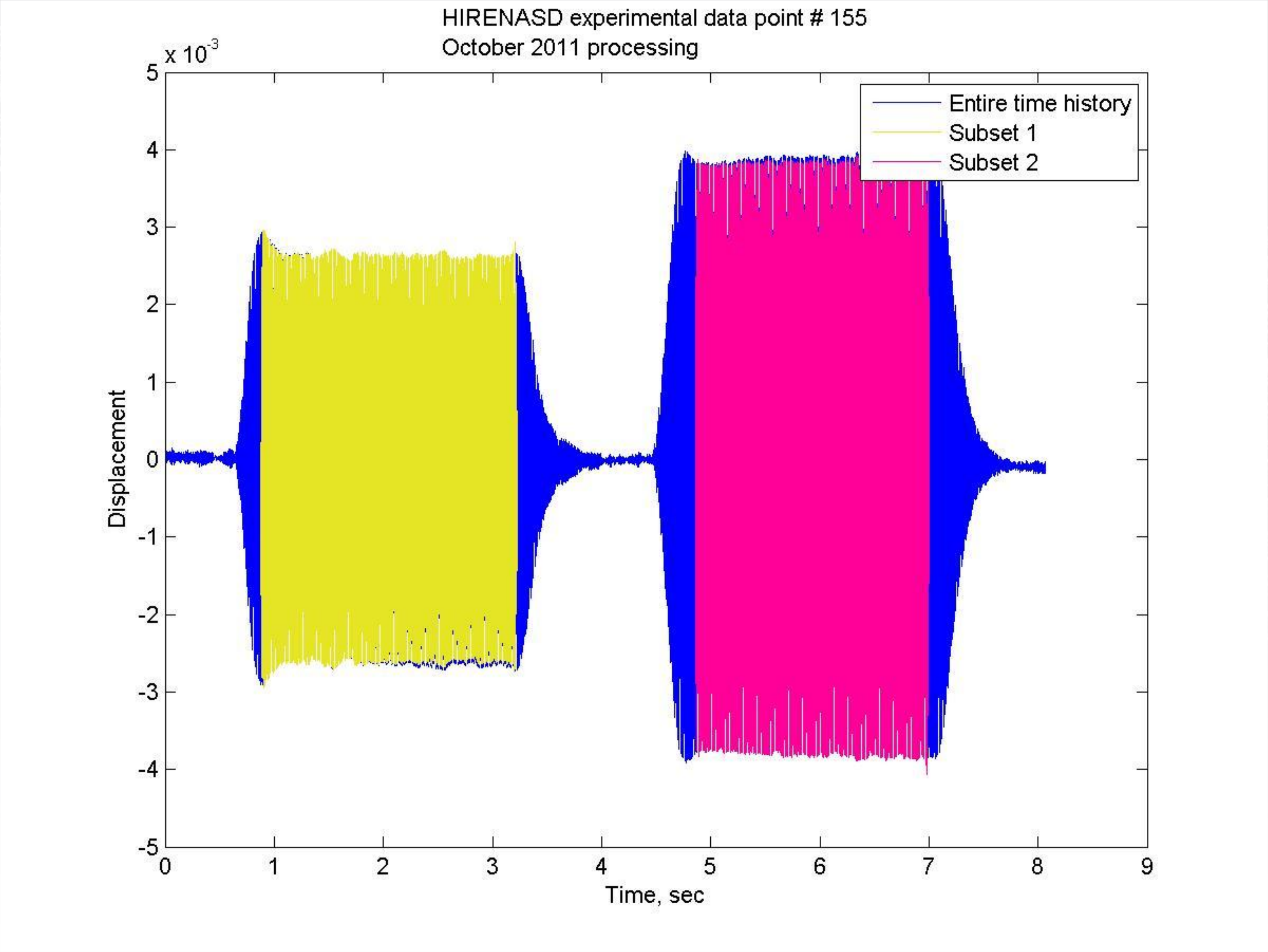

# HIRENASD FRF, subset effects

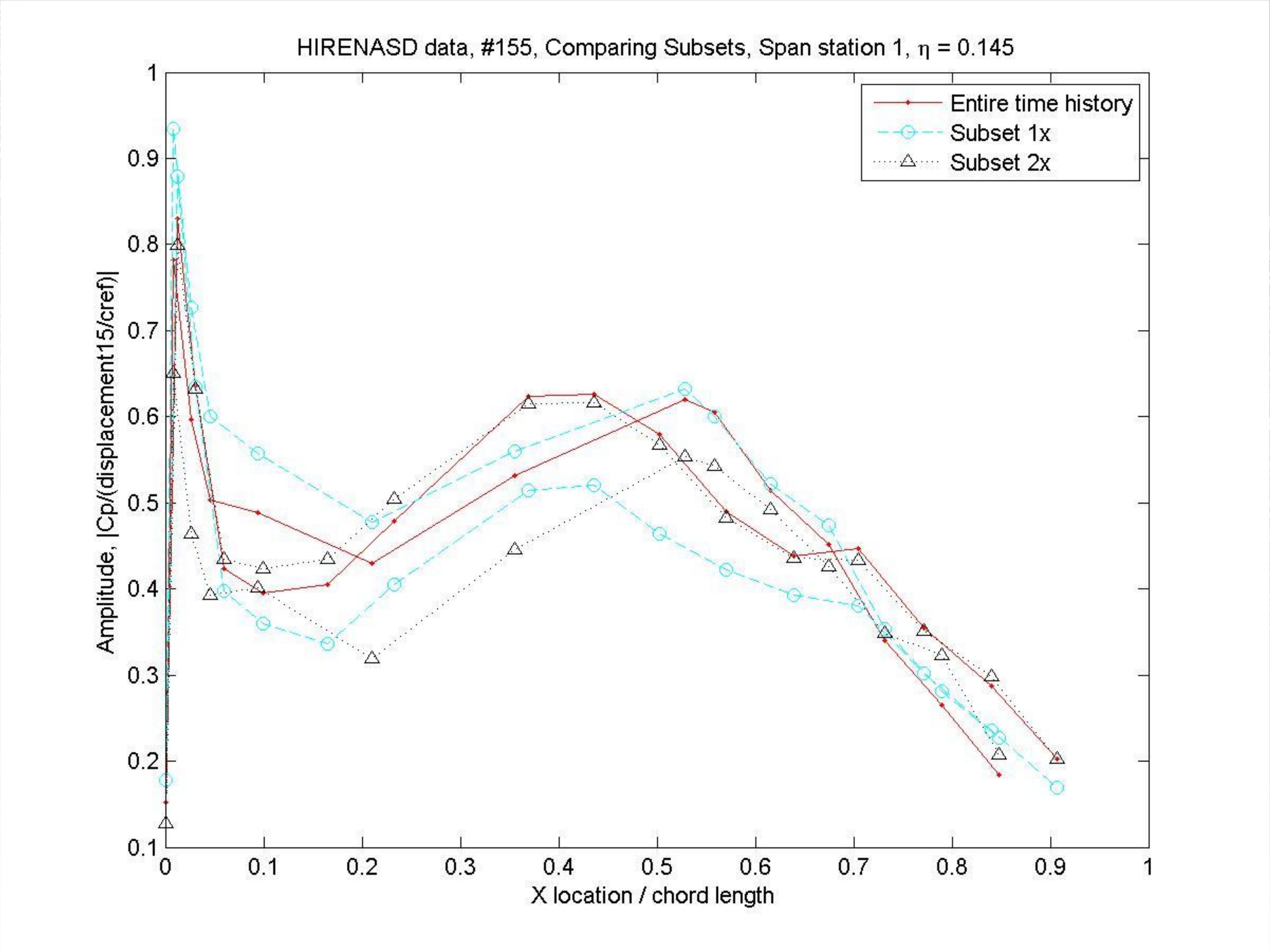

# HIRENASD data subset used for unsteady data reduction- Excitation signal

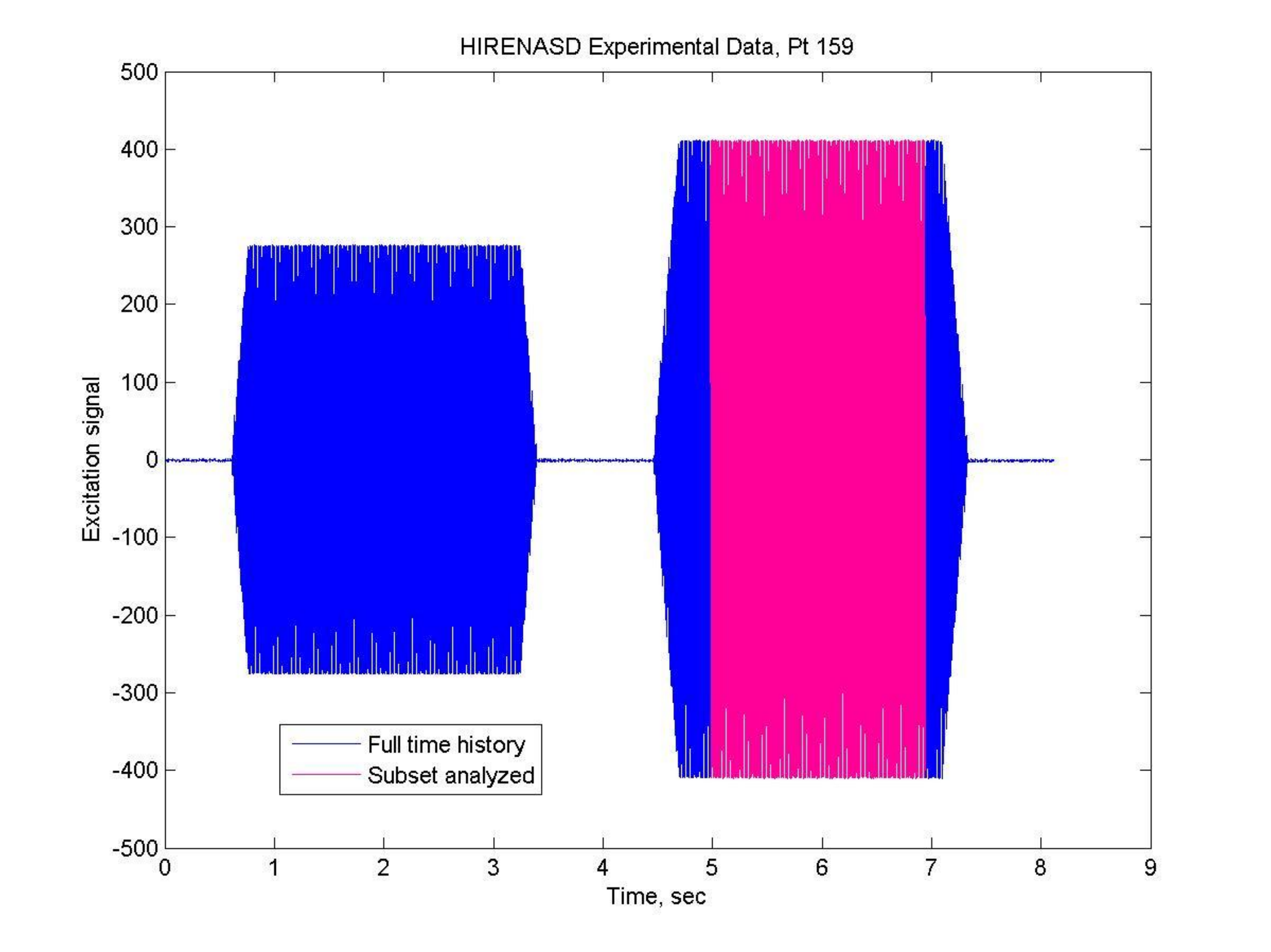

# HIRENASD data subset used for unsteady data reduction- Acceleration signal

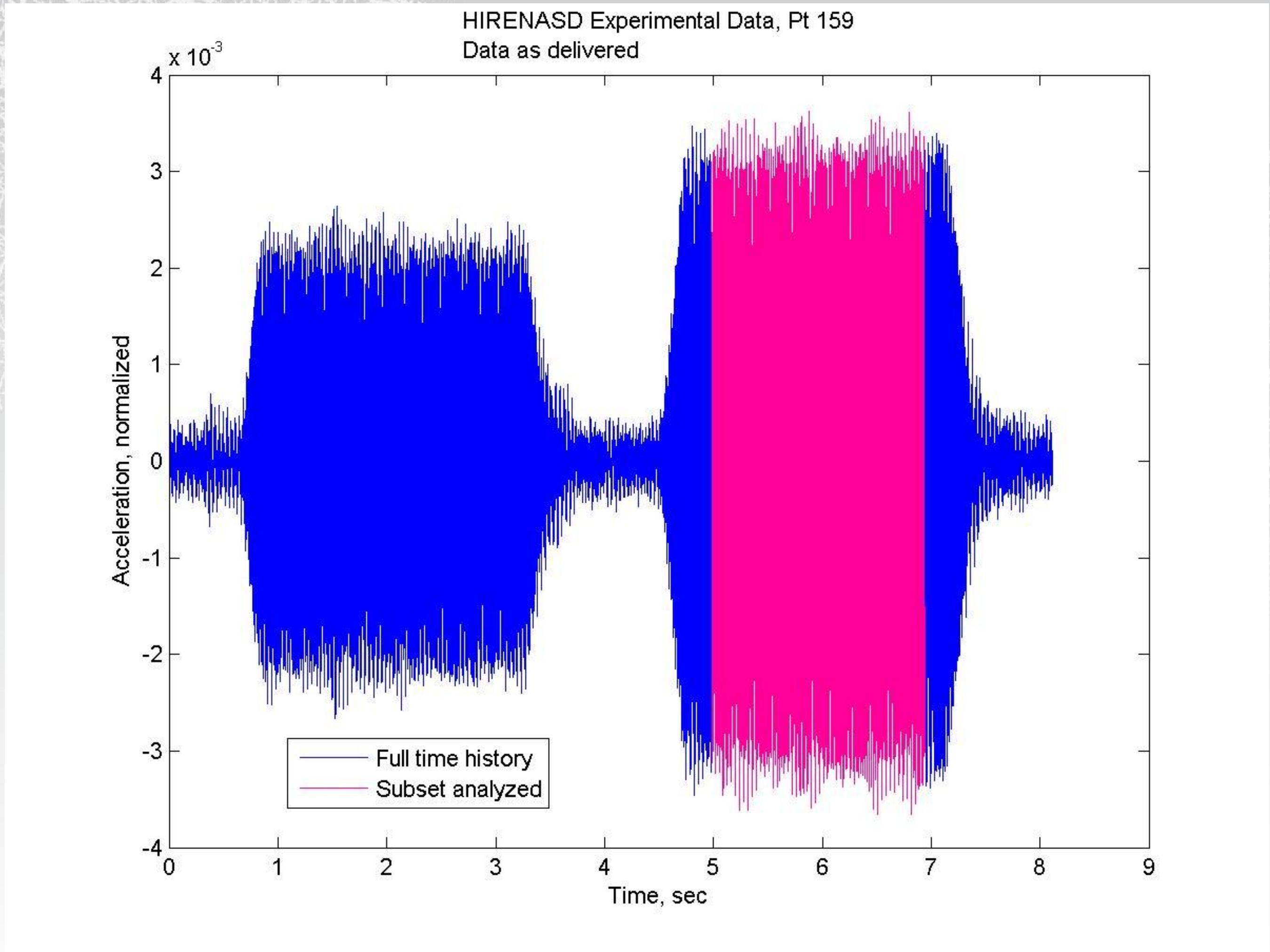

# *Fourier analysis: analysis time length varied by 1 sample increments to determine block size*

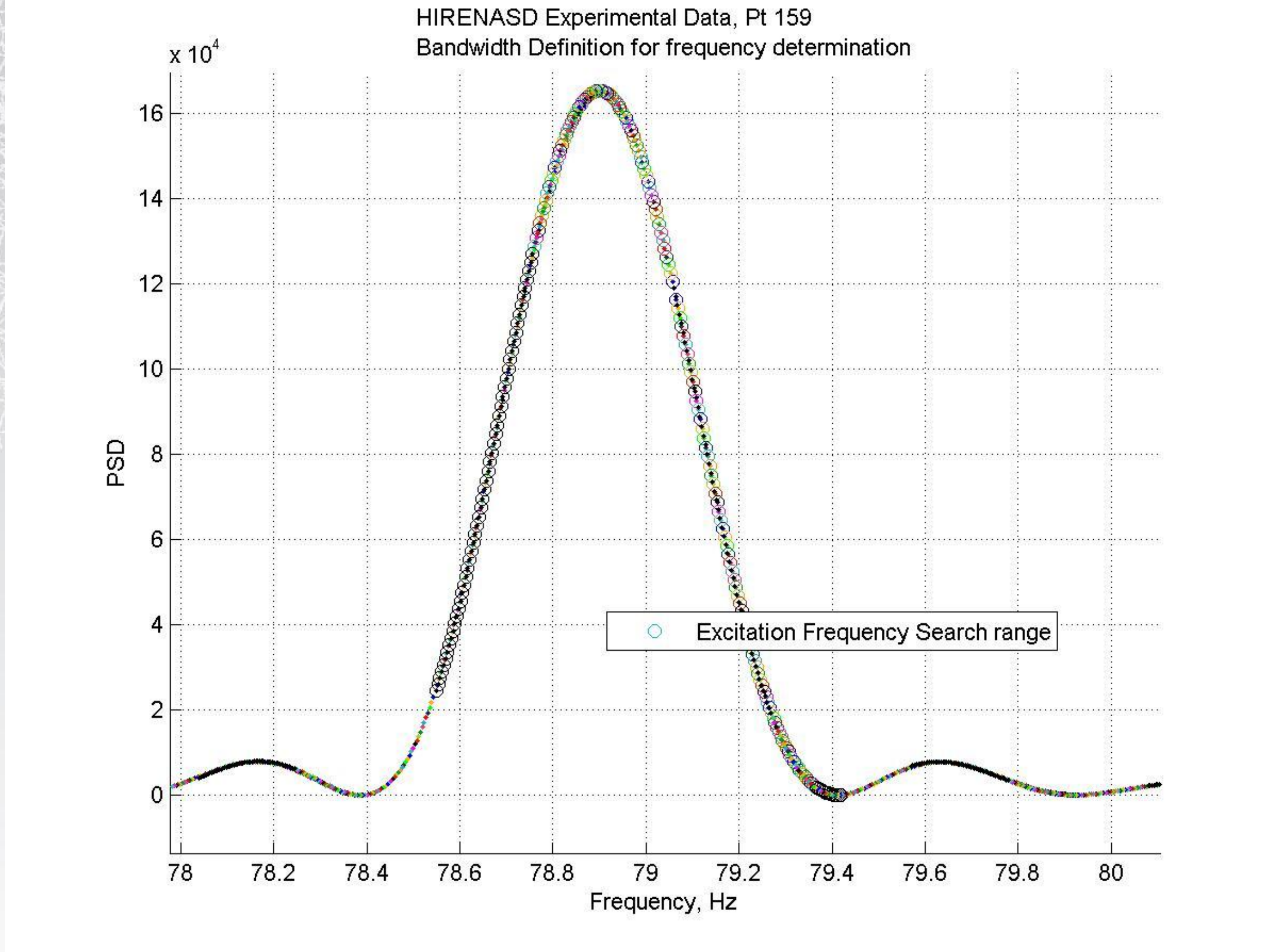


Power spectral density function of excitation signal:
Analysis block size determined by minimum standard deviation among ensembles

# Frequency response functions for several transducers

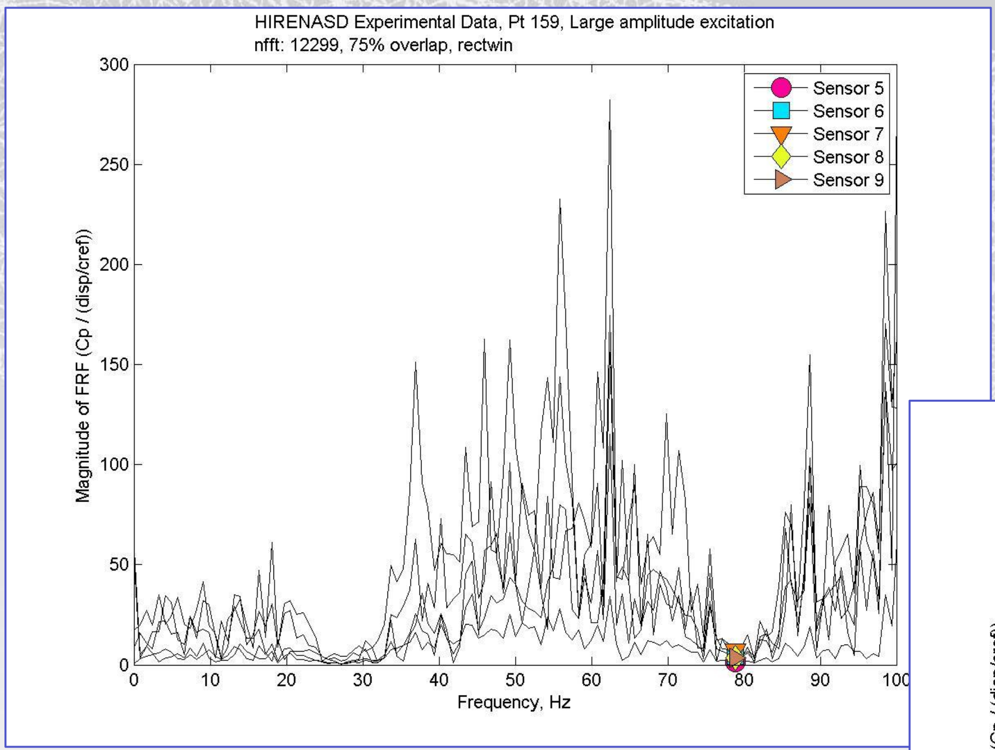


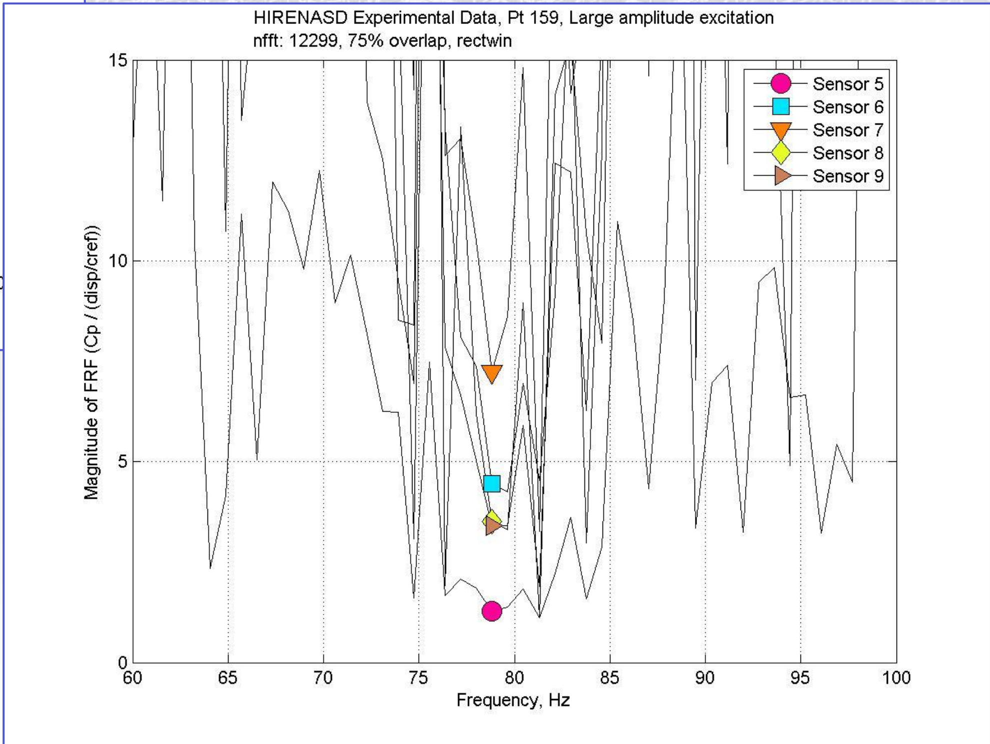

# Coherence for corresponding transducers

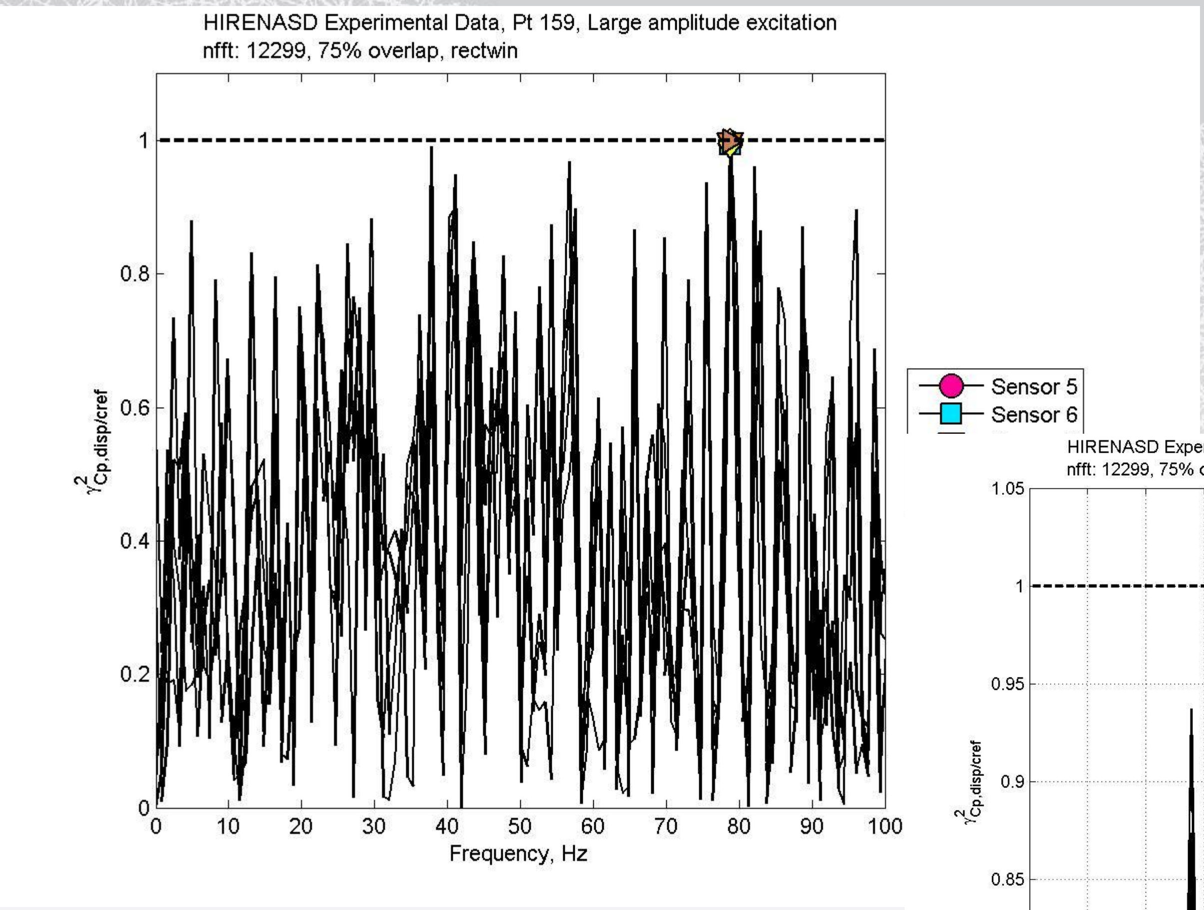


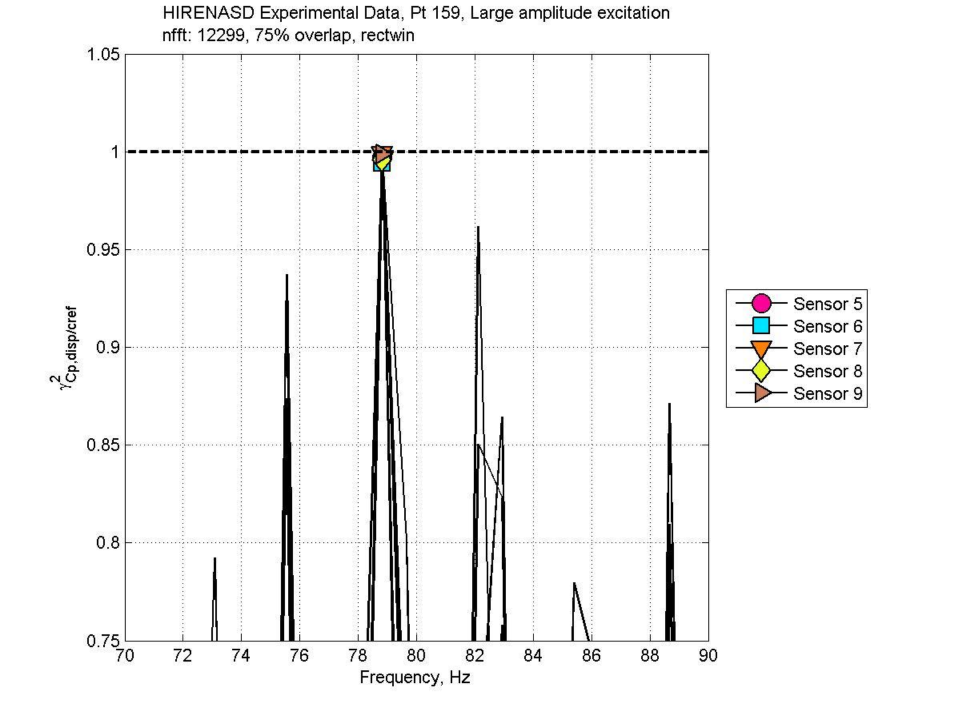

# Frequency response function at excitation frequency: all sensors at 1 span station

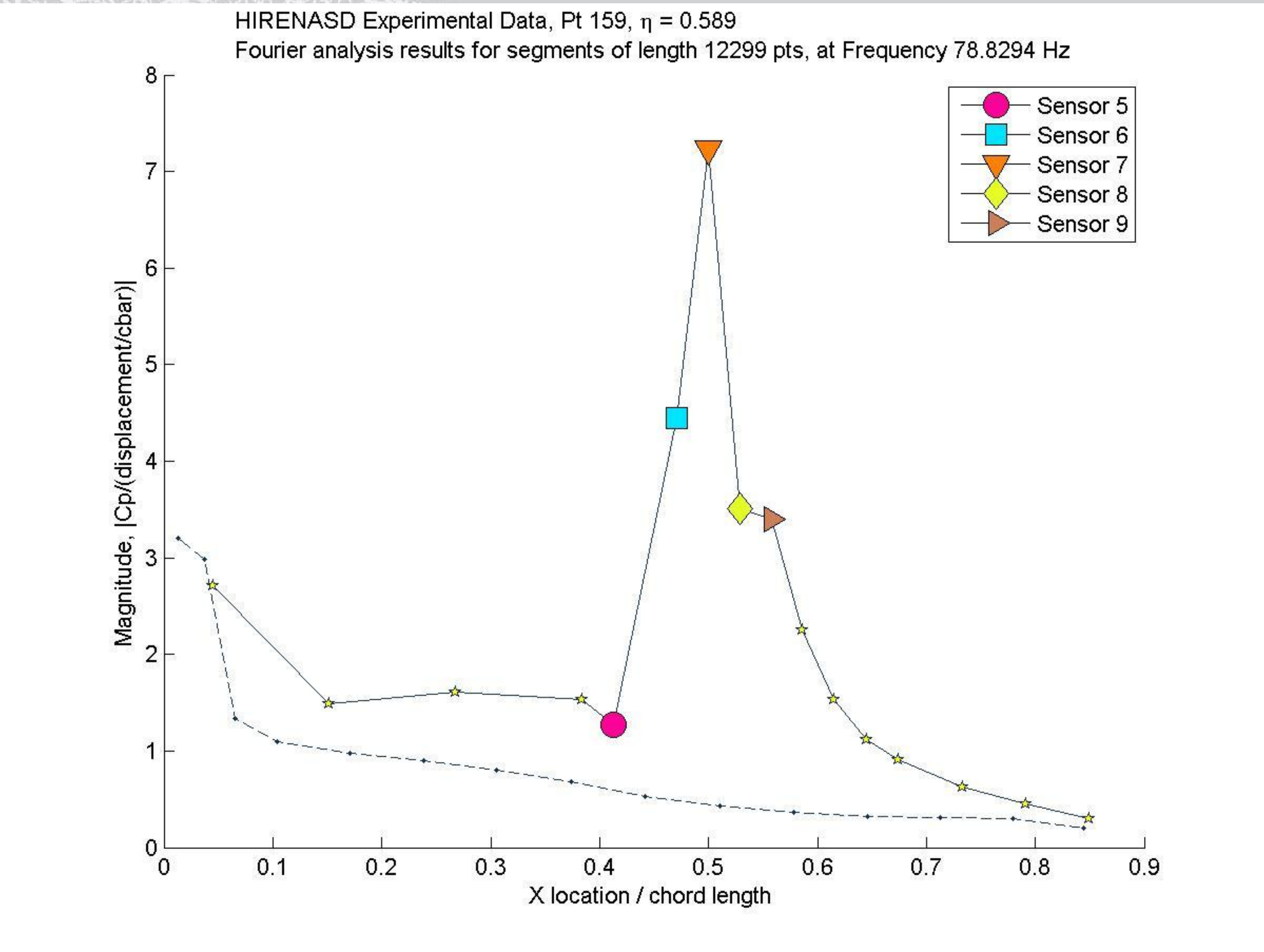

# Corresponding coherence

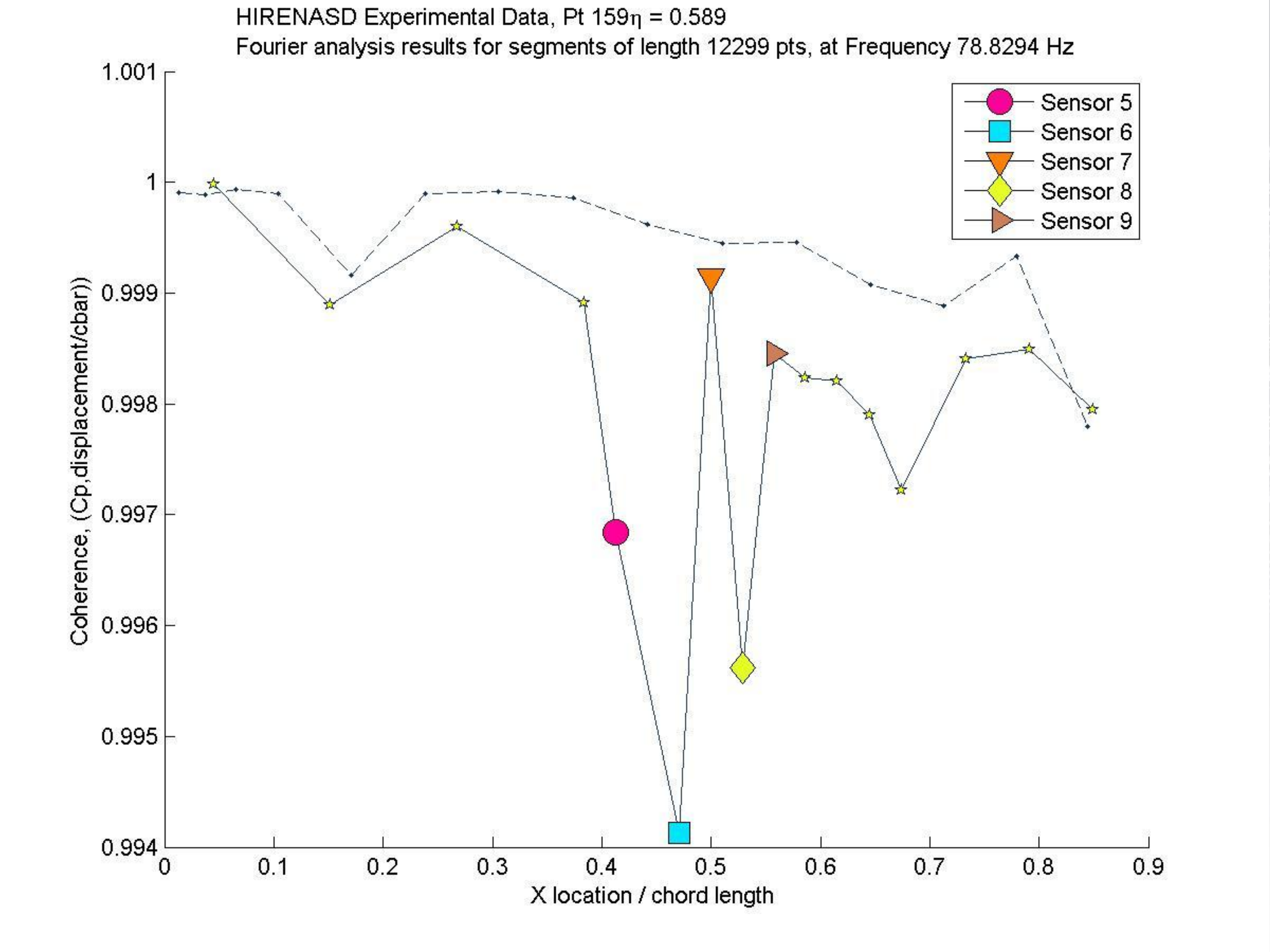

# *Example of dynamic comparison data: HIRENASD Frequency Responses at 2nd Bending Mode Frequency (78.9 Hz)*

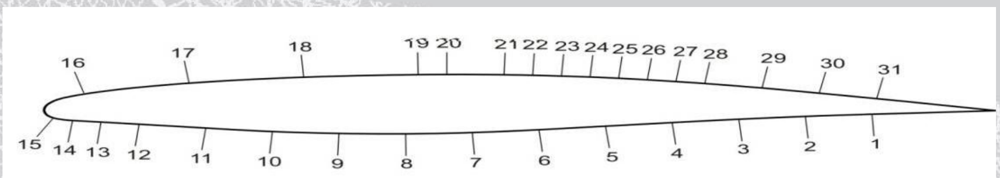


Cp(x)/displacement

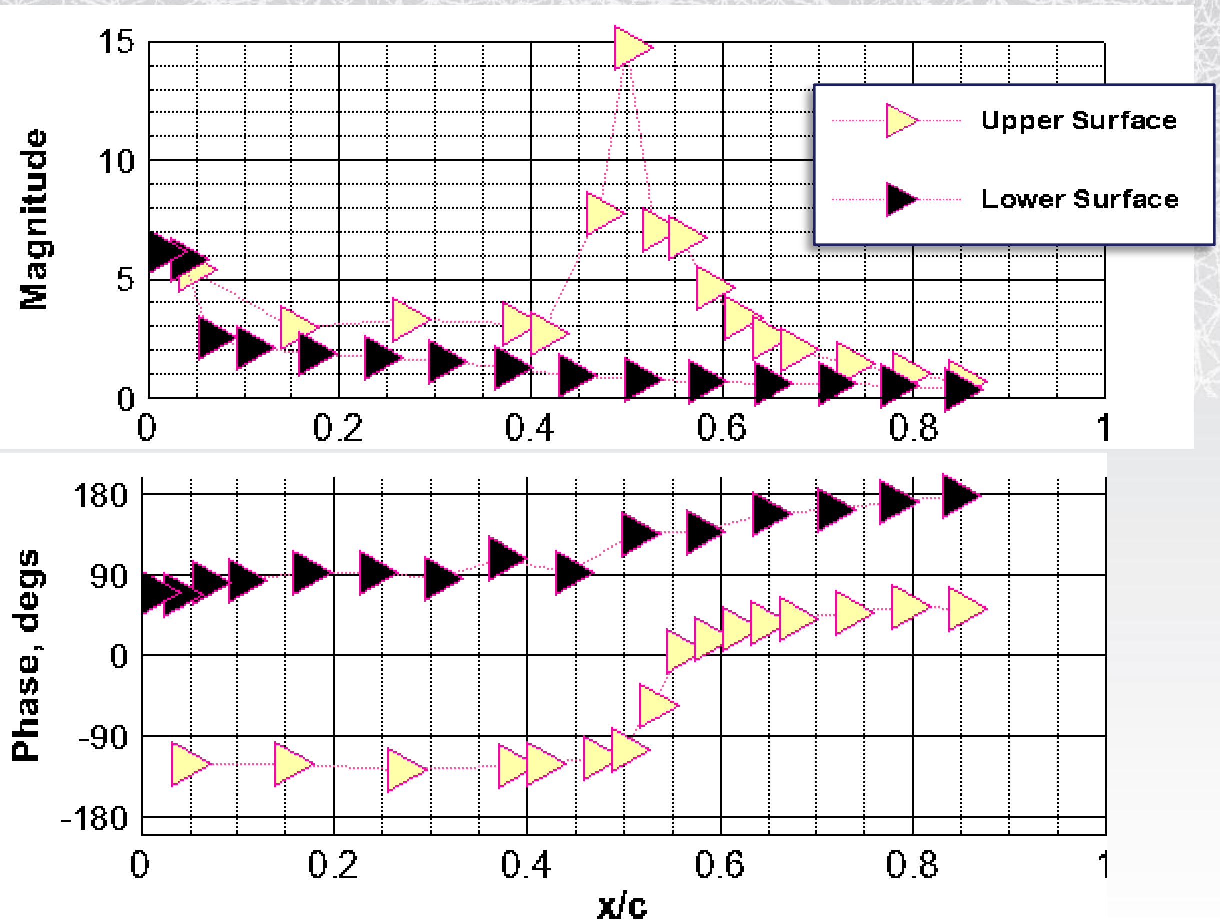


Pressure coefficients at span station 4 due to displacement at location (15,1)

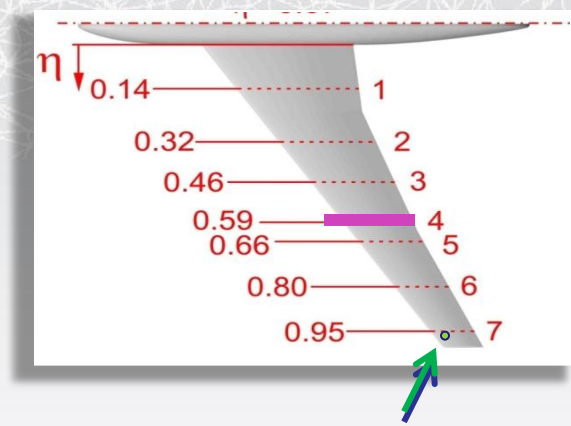


Reference quantity: Displacement at location (15,1)

HIRENASD Exp Data, Pt 159 : FRFs of Cp due to displacement, frequency = 78.8294 Hz

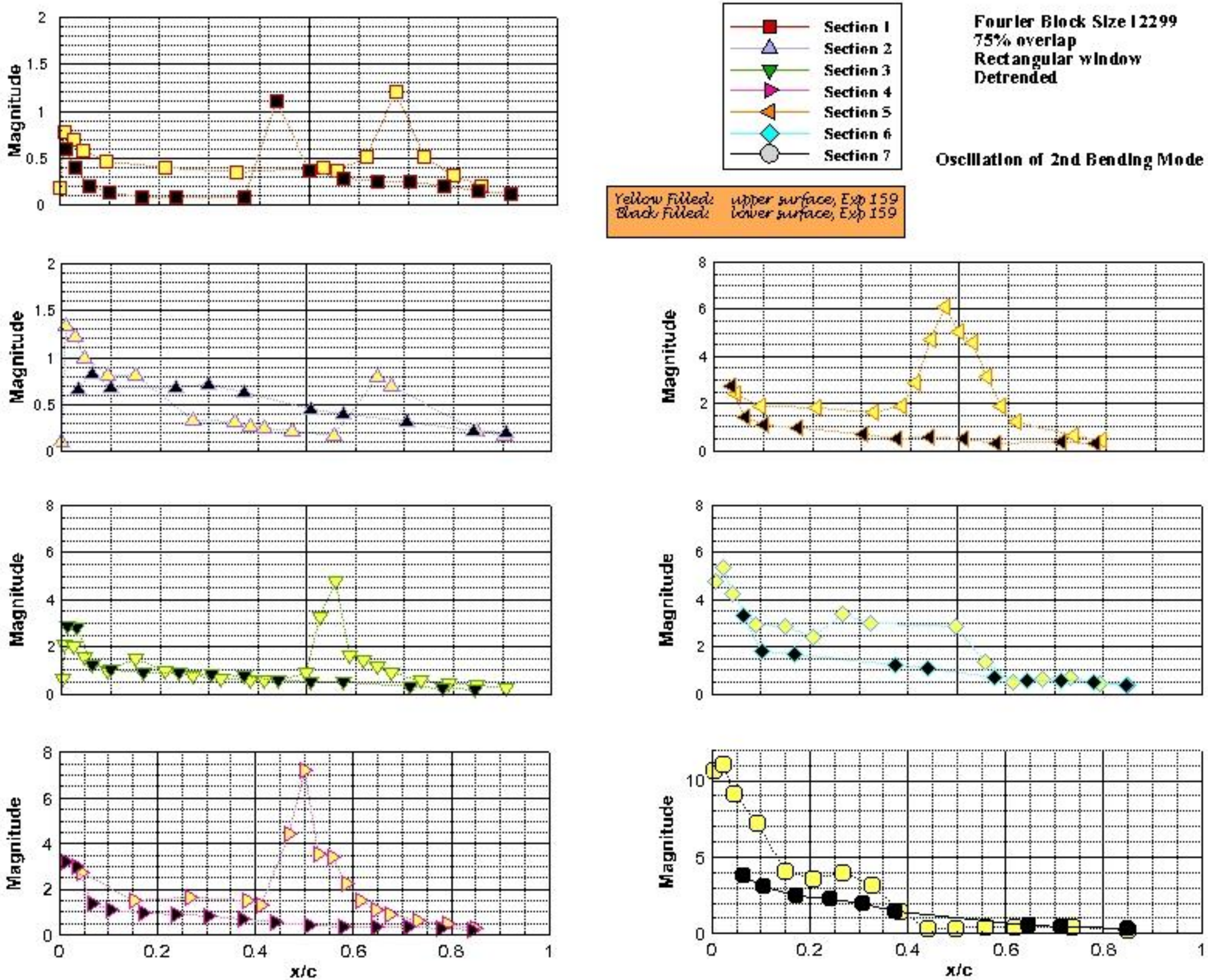

## *CFD displacement amplitude calculation*

- Fourier analysis of integrated displacement

# HIRENASD data, displacement signal

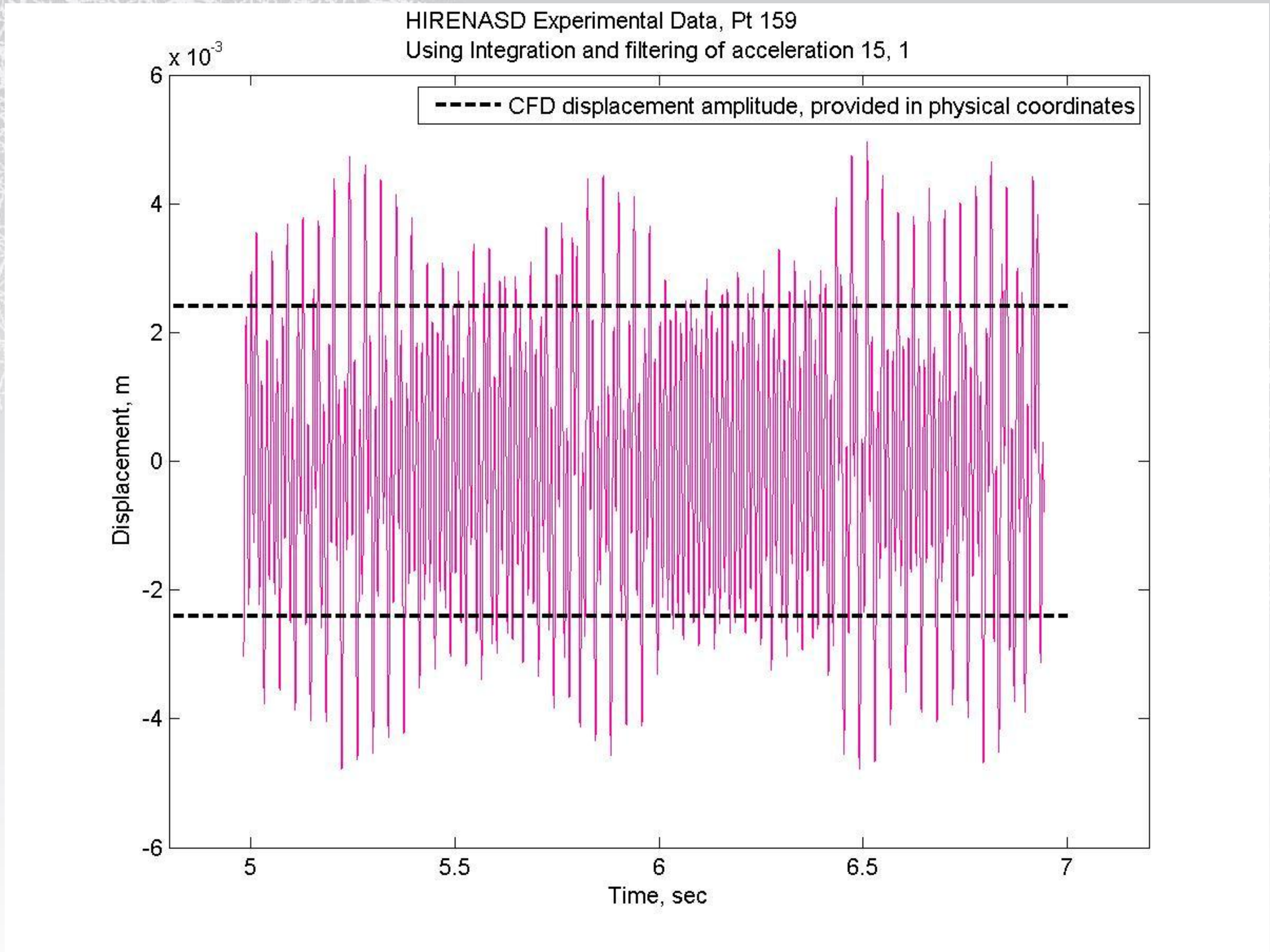

# HIRENASD data, Fourier analysis of displacement signal

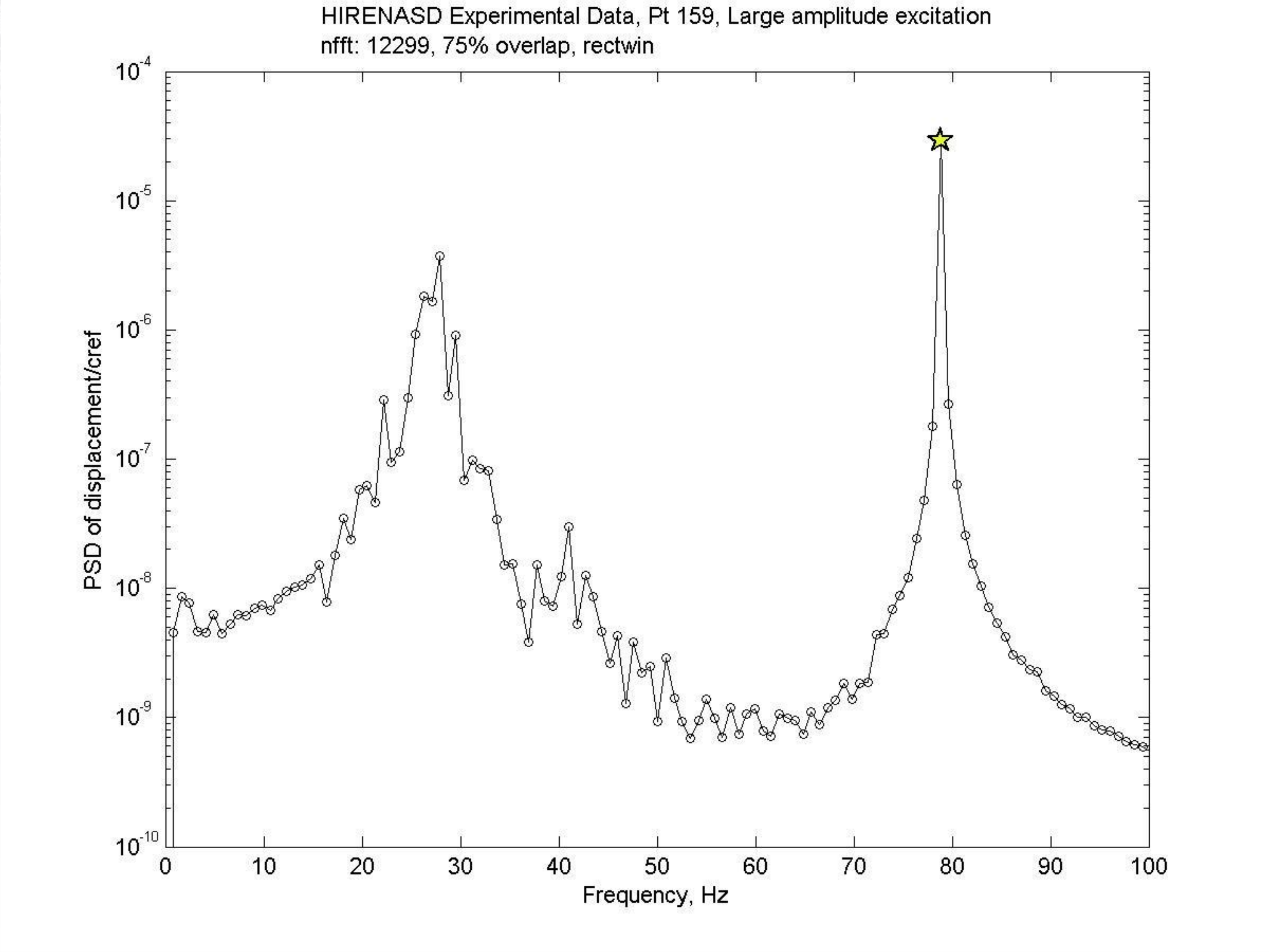

# HIRENASD Response Amplitudes

- Updated information:
  - Amplitude of excitations for 2nd bending modes for each of the 3 unsteady cases, extracted from the experimental data:

| Exp Test Pt | 159 | 271 | 155 |
|---|---|---|---|
| Mach # | 0.8 | 0.8 | 0.7 |
| $Re_c$ | 7M | 23.5M | 7M |
| Amplitude (mm) | 2.4 | 0.90 | 2.0 |
| Frequency (Hz) | 78.9 | 80.4 | 79.3 |

For those analysts using strictly forced oscillations (similar methodology to RSW and BSCW), it is recommended that they use the frequencies extracted from the experimental data at the test conditions, as given in the table above. It is recommended that they oscillate the model in the 2nd bending mode shape as given by the finite element model.

For those analysts who are performing a coupled aeroelastic analysis, proximity of the oscillatory frequency to the modal frequency may be a dominant effect, and these frequencies are likely not exactly correct. The next slide contains a summary of the air-off natural frequencies of the 2nd bending mode. The first 2 columns show the experimental data; the last column shows the current finite element model frequency.

# Additional Information

# Comparison Data Matrix

| CONFIGURATION | REQUIRED CALCULATIONS | | | |
|---|---|---|---|---|
| | GRID CONVERGENCE STUDIES | TIME CONVERGENCE STUDIES | STEADY CALCULATIONS | DYNAMIC CALCULATIONS |
| Steady-Rigid Cases (RSW, BSCW) | $C_L$, $C_D$, $C_M$ vs. $N^{-2/3}$ ✓ | n/a | • Mean $C_p$ vs. x/c ✓<br>• Means of $C_L$, $C_D$, $C_M$ ✓ | n/a |
| Steady-Aeroelastic Cases (HIRENASD) | $C_L$, $C_D$, $C_M$ vs. $N^{-2/3}$ ✓ | n/a | • Mean $C_p$ vs. x/c ✓<br>• Means of $C_L$, $C_D$, $C_M$ ✓<br>• Vertical displacement vs. chord ✓<br>• Twist angle vs. span ✓ | n/a |
| Forced Oscillation Cases (all configurations) | • Magnitude and Phase of $C_L$, $C_D$, $C_M$ vs. $N^{-2/3}$ at excitation frequency ✓ | • Magnitude and Phase of $C_L$, $C_D$, $C_M$ vs. $\Delta t$ at excitation frequency ✓ | n/a | • Magnitude and Phase of $C_p$ vs. x/c at span stations corresponding to transducer locations ✓<br>• Magnitude and Phase of $C_L$, $C_D$, $C_M$ at excitation frequency ✓<br>• Time histories of $C_p$'s at a selected span station for two upper- and two lower-surface transducer locations |

# RSW – BSCW – HIRENASD
# $c_p$ Time Histories

One chart per configuration

*At chord locations where upper-surface $c_p$ is peak as determined by -*

*- Experiment* *- Computation*

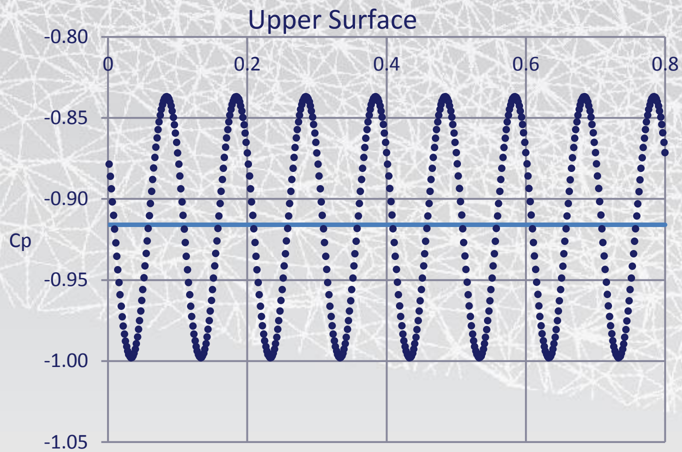


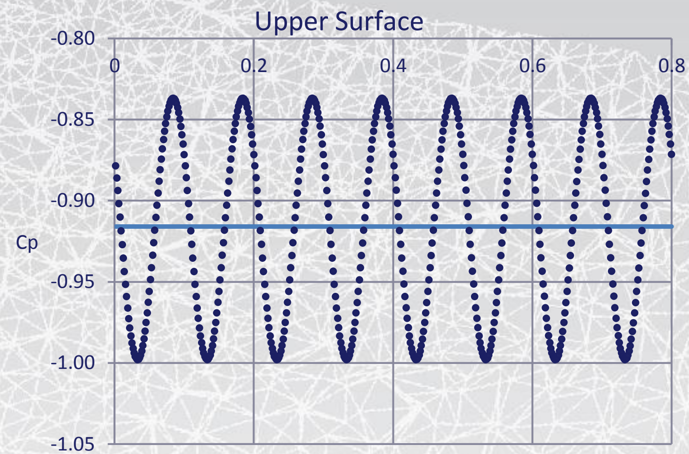


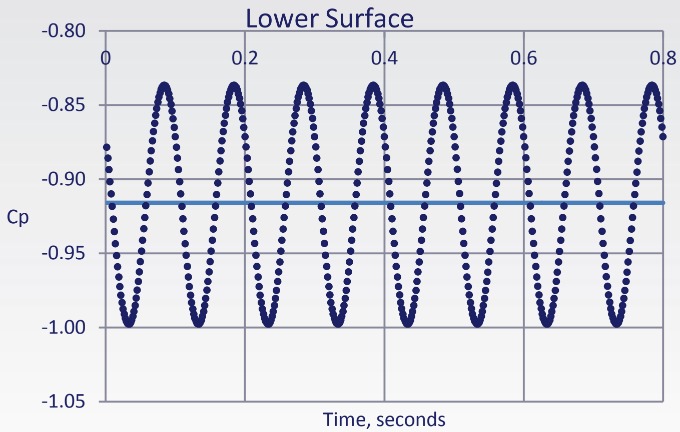


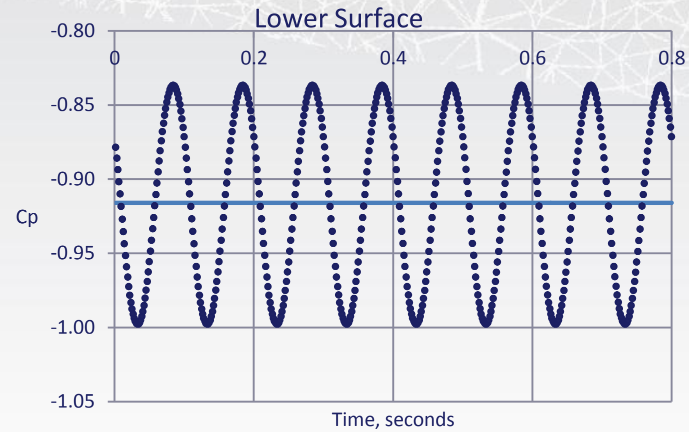


The purpose of this series of charts is to look for evidence of nonlinearities in the computational aeroelastic solutions.

For each configuration, for two specified pairs of points within a specified span station, time histories of analytically-predicted $C_p$'s are plotted:

1. The first pair is comprised of the upper- and lower-surface $C_p$'s at the chordwise position where fourier analysis of the experimental data shows the experimental upper-surface $C_p$ to be at its peak;
2. The second pair is comprised of the upper- and lower-surface $C_p$'s at the chordwise position where fourier analysis of the analytical predictions shows the analytical upper-surface $C_p$ to be at its peak.

*Pawel RSW calculation, coarse grid, eta=0.309*
*Alpha = 2deg, Unsteady, f=10Hz, theta=1deg*

# Comparison Data Matrix

| CONFIGURATION | REQUIRED CALCULATIONS | | | |
|---|---|---|---|---|
| | GRID CONVERGENCE STUDIES | TIME CONVERGENCE STUDIES | STEADY CALCULATIONS | DYNAMIC CALCULATIONS |
| Steady-Rigid Cases (RSW, BSCW) | $C_L$, $C_D$, $C_M$ vs. $N^{-2/3}$ | n/a | • Mean $C_p$ vs. x/c<br>• Means of $C_L$, $C_D$, $C_M$ | n/a |
| Steady-Aeroelastic Cases (HIRENASD) | $C_L$, $C_D$, $C_M$ vs. $N^{-2/3}$ | n/a | • Mean $C_p$ vs. x/c<br>• Means of $C_L$, $C_D$, $C_M$<br>• Vertical displacement vs. chord<br>• Twist angle vs. span | n/a |
| Forced Oscillation Cases (all configurations) | • Magnitude and Phase of CL, CD, CM vs. $N^{-2/3}$ at excitation frequency | • Magnitude and Phase of $C_L$, $C_D$, $C_M$ vs. $\Delta t$ at excitation frequency | n/a | • Magnitude and Phase of $C_p$ vs. x/c at span stations corresponding to transducer locations<br>• Magnitude and Phase of $C_L$, $C_D$, $C_M$ at excitation frequency<br>• Time histories of $C_p$'s at a selected span station for two upper- and two lower-surface transducer locations |

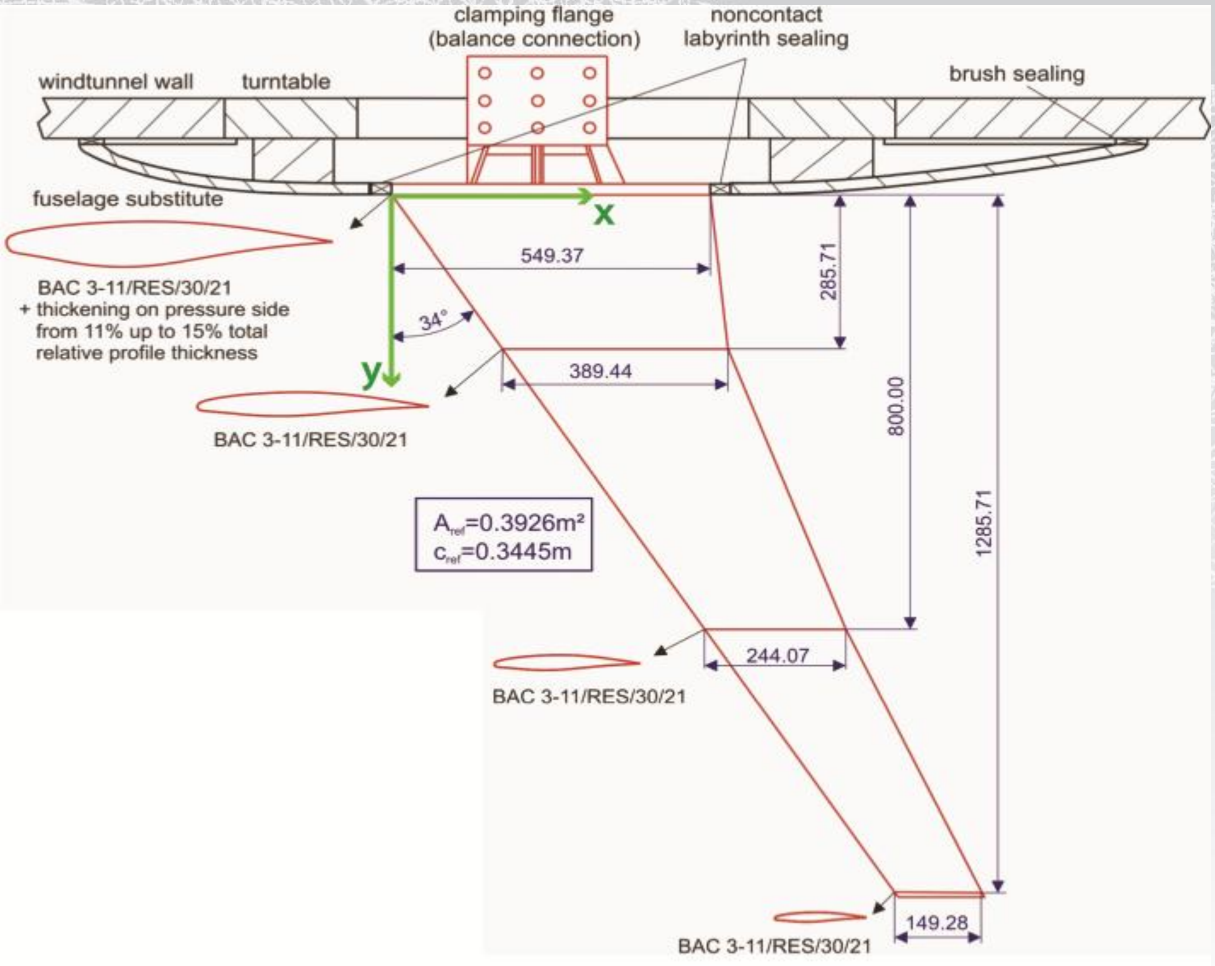

clamping flange
(balance connection)
noncontact
labyrinth sealing
windtunnel wall
turntable
brush sealing
fuselage substitute
x
y
549.37
285.71
800.00
1285.71
34°
389.44
BAC 3-11/RES/30/21
+ thickening on pressure side
from 11% up to 15% total
relative profile thickness
BAC 3-11/RES/30/21
A_ref=0.3926m²
c_ref=0.3445m
244.07
BAC 3-11/RES/30/21
149.28
BAC 3-11/RES/30/21

# Static Test Results, Reynolds Number Varied

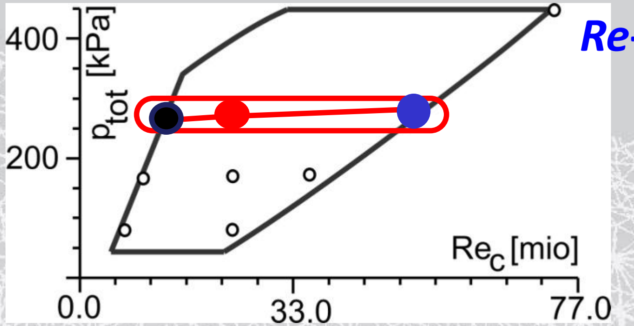


***Re*-Variation:** Influence on lift and drag

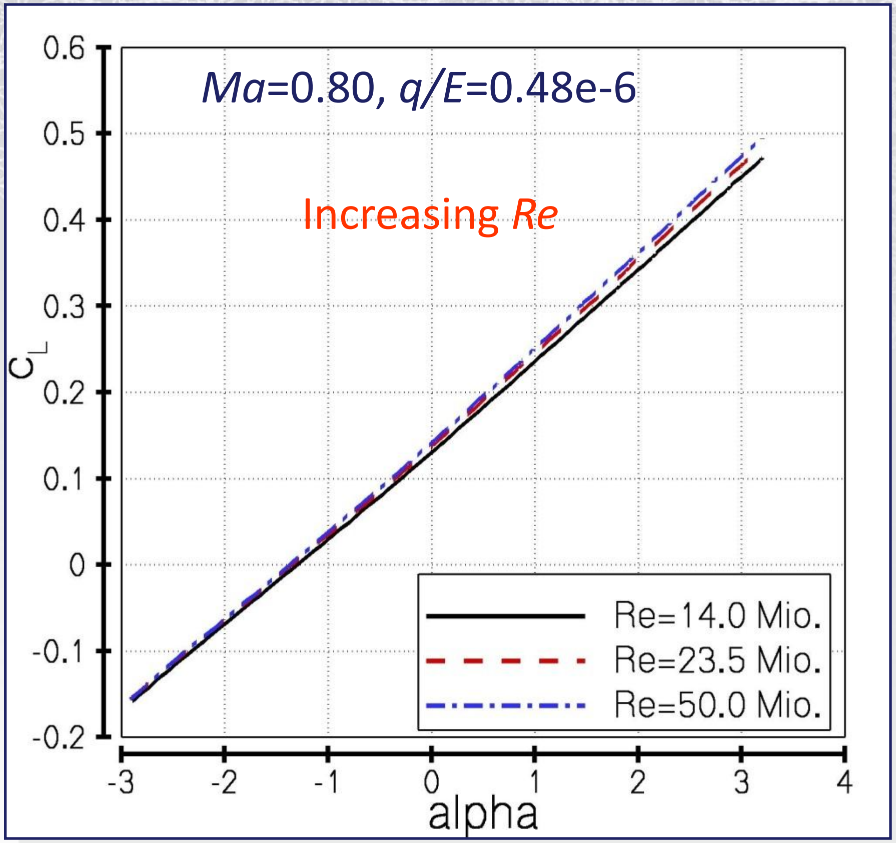


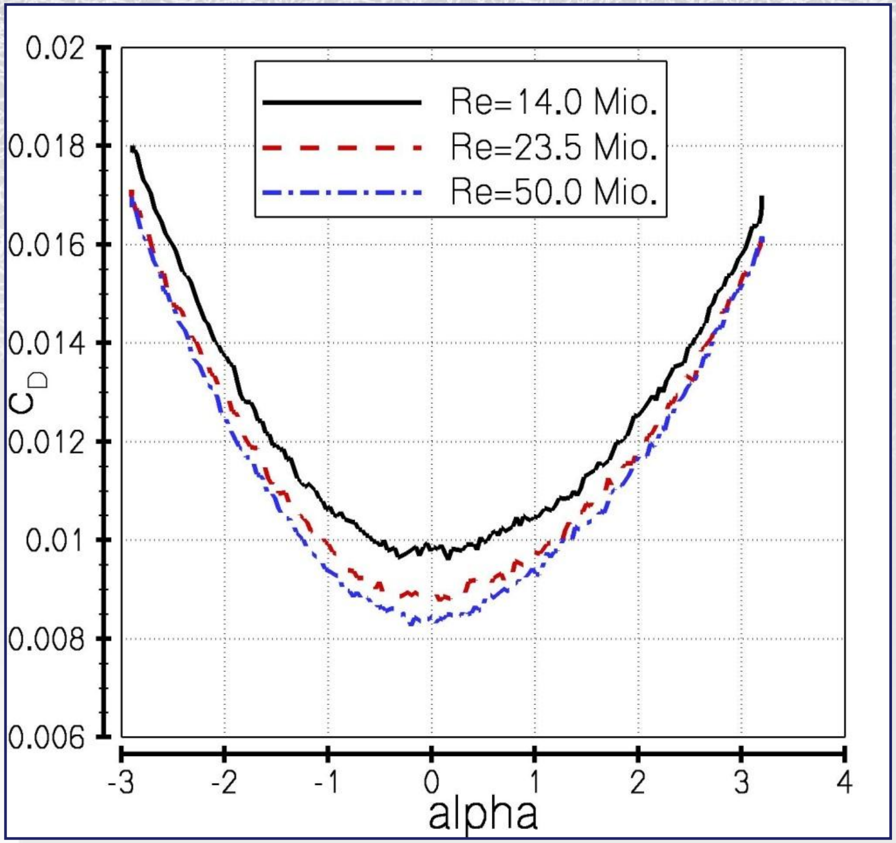

# Additional things about the BSCW data

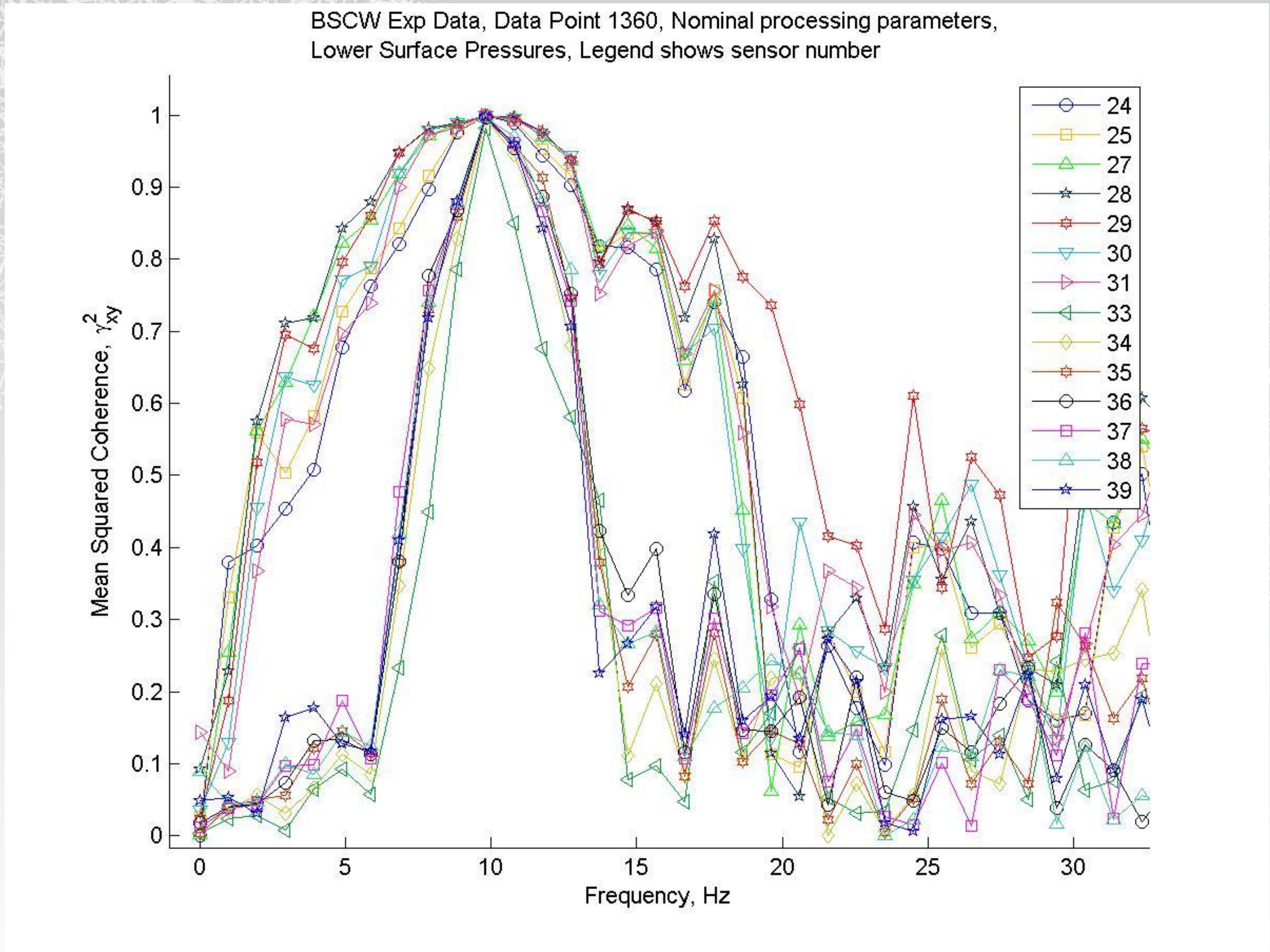

BSCW Exp Data, Data Point 1360, Nominal processing parameters,
Lower Surface Pressures, Legend shows sensor number
Mean Squared Coherence, $\gamma^2_{xy}$
Frequency, Hz
0
0.1
0.2
0.3
0.4
0.5
0.6
0.7
0.8
0.9
1
5
10
15
20
25
30
24
25
27
28
29
30
31
33
34
35
36
37
38
39

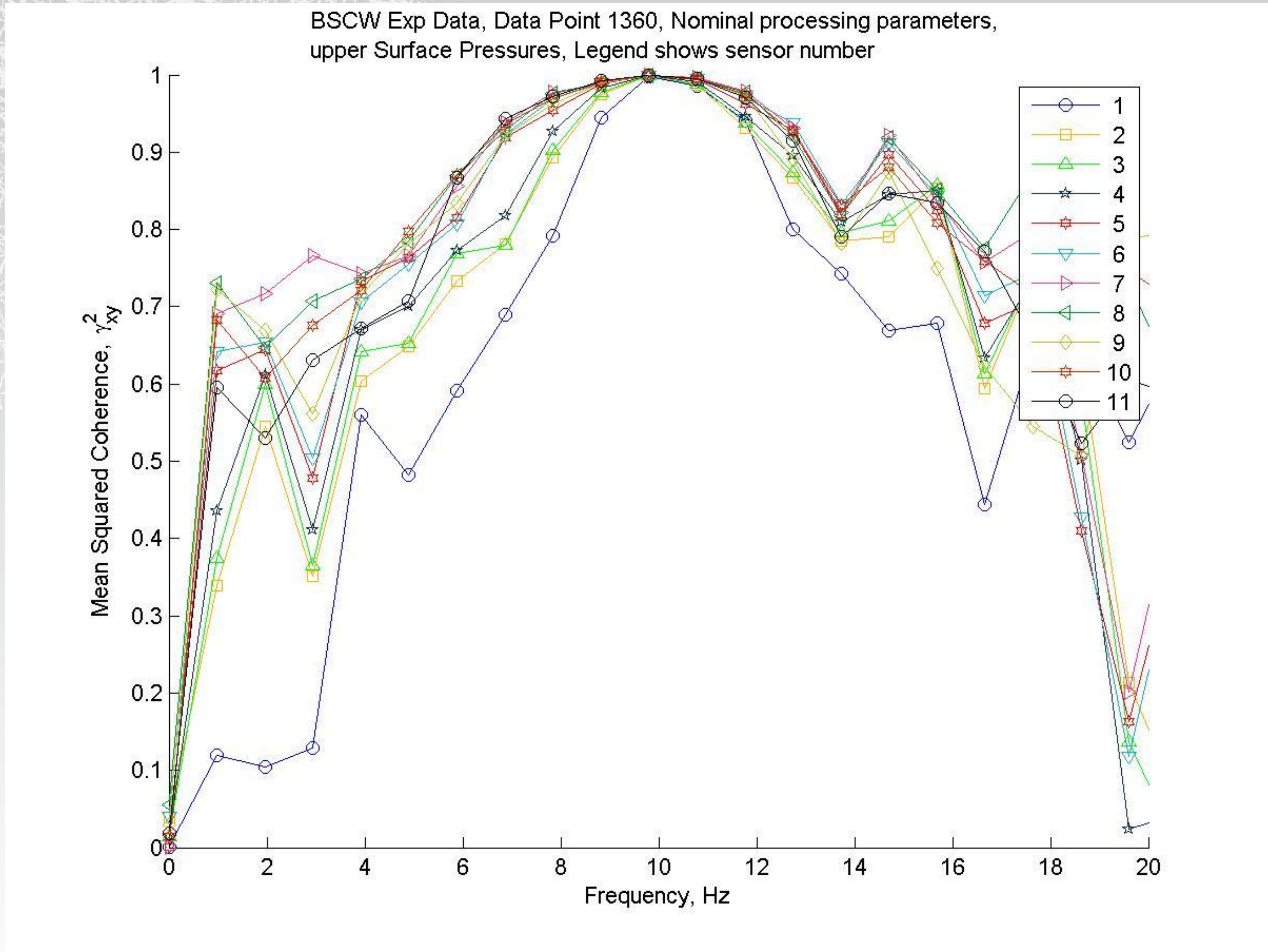
BSCW Exp Data, Data Point 1360, Nominal processing parameters,
upper Surface Pressures, Legend shows sensor number
Mean Squared Coherence, $\gamma^2_{xy}$
Frequency, Hz
0
0.1
0.2
0.3
0.4
0.5
0.6
0.7
0.8
0.9
1
2
4
6
8
10
12
14
16
18
20
3
5
7
9
11

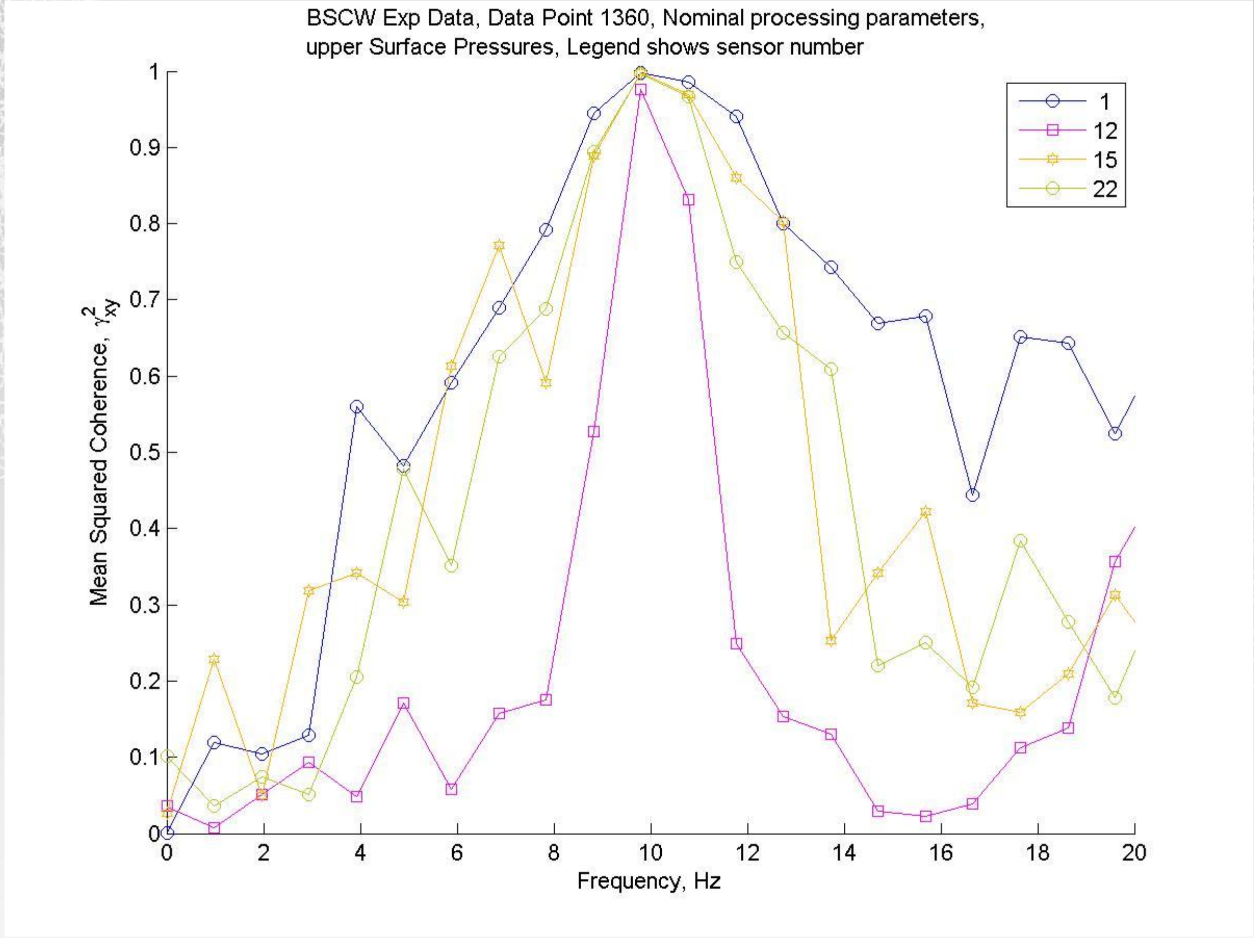
BSCW Exp Data, Data Point 1360, Nominal processing parameters,
upper Surface Pressures, Legend shows sensor number
Mean Squared Coherence, $\gamma^2_{xy}$
Frequency, Hz
1
12
15
22
0
0.1
0.2
0.3
0.4
0.5
0.6
0.7
0.8
0.9
1
0
2
4
6
8
10
12
14
16
18
20

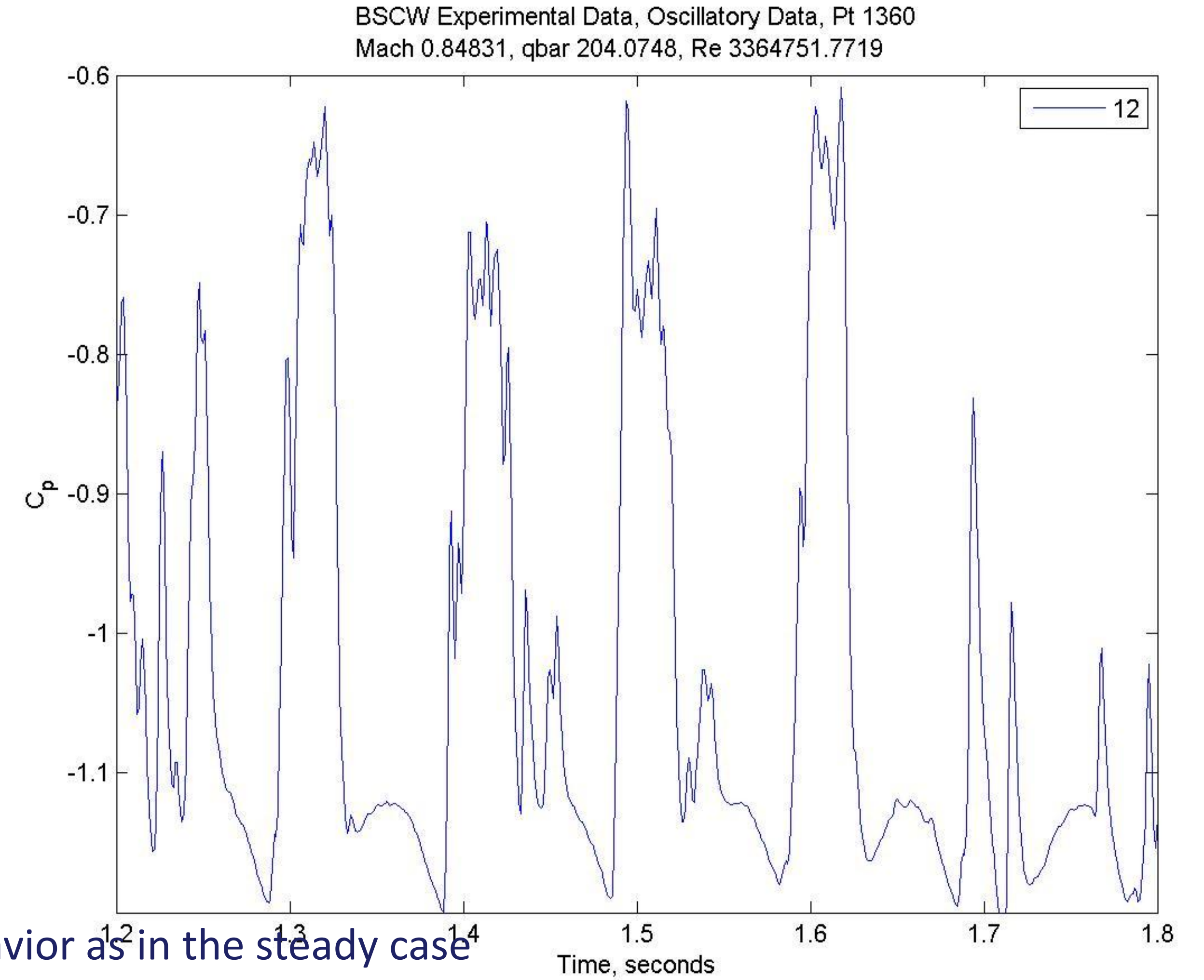


Ceiling behavior as in the steady case
Excitation frequency in evidence for half cycles

Excursion of shock across transducer (past transducer towards leading edge )
Occurs principally during the first ½ cycle of excitation shown

# Frequency content of the excursions?

Nothing stands out when I look
At these to differentiate
Sensor 12 from the ones before and
After it…

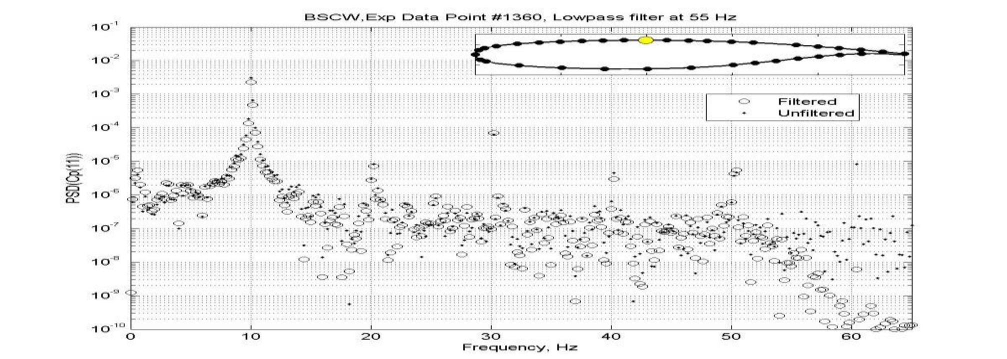


Sensor #11

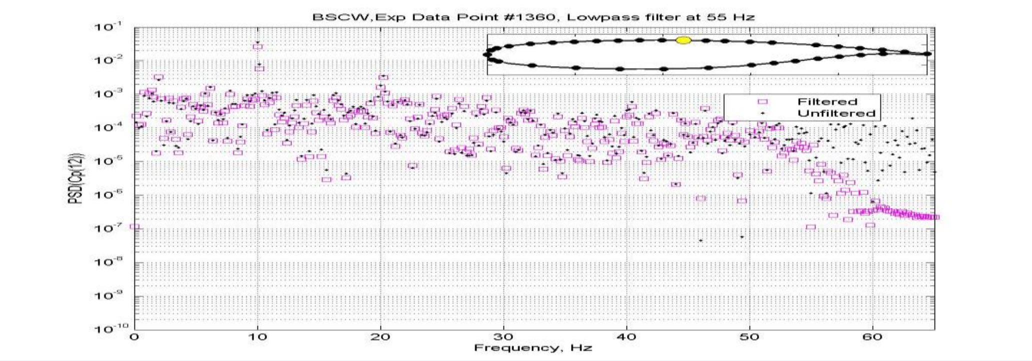


Sensor #12

Sensor #13

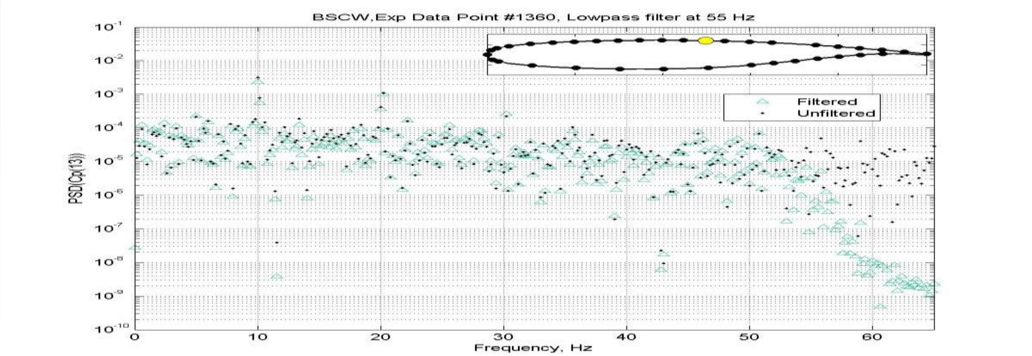

# BSCW Static Data:
# Steady Shock Location

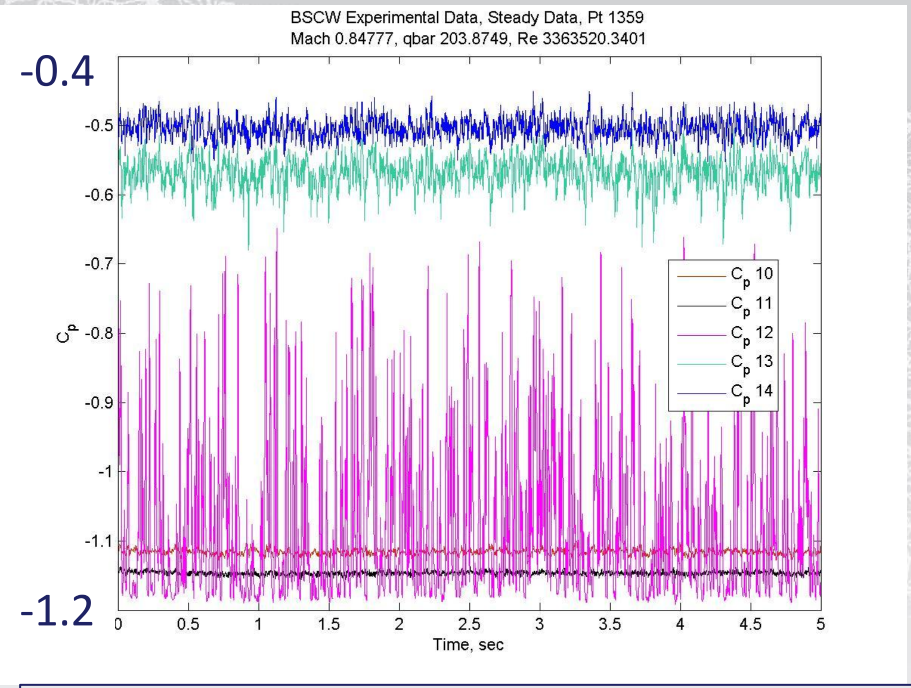


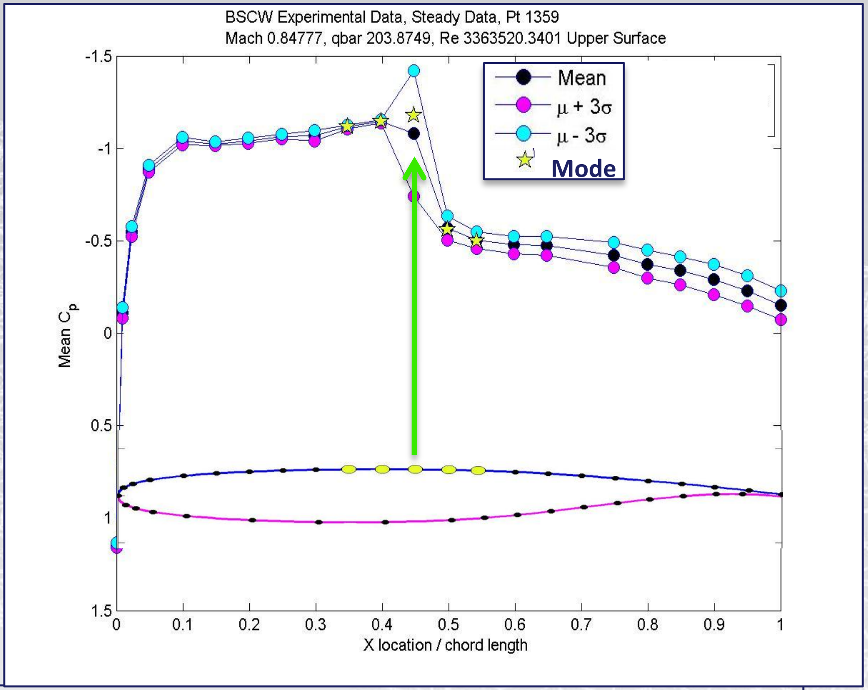


**Location: just barely aft of upper surface transducer #12, x/c (12) = 0.448**

**(Note: x/c (13) = 0.498)**

Upper surface pressure transducer 12: magenta data plot

- Pressure floor at -1.17, i.e. it is bounded by -1.17
- No well-defined, repeated ceiling value
- Not sinusoidal

Expected pressure change across the shock:

- large negative pressure ahead of the shock;
- reduced negative pressure aft of the shock

Actual shock location is suspected to be just aft of this transducer location: the value oscillates to a higher pressure (aft of shock) as the shock moves

Sensors towards leading edge (#10 and #11) have values near the minimum of #12

Sensors towards trailing edge (#13 and #14) have values beyond the maximum of #12

**Simple interpretation: the sensor's preferred value reflects pressure ahead of shock, rather than aft of it.**

# Standard Deviation of Static Data

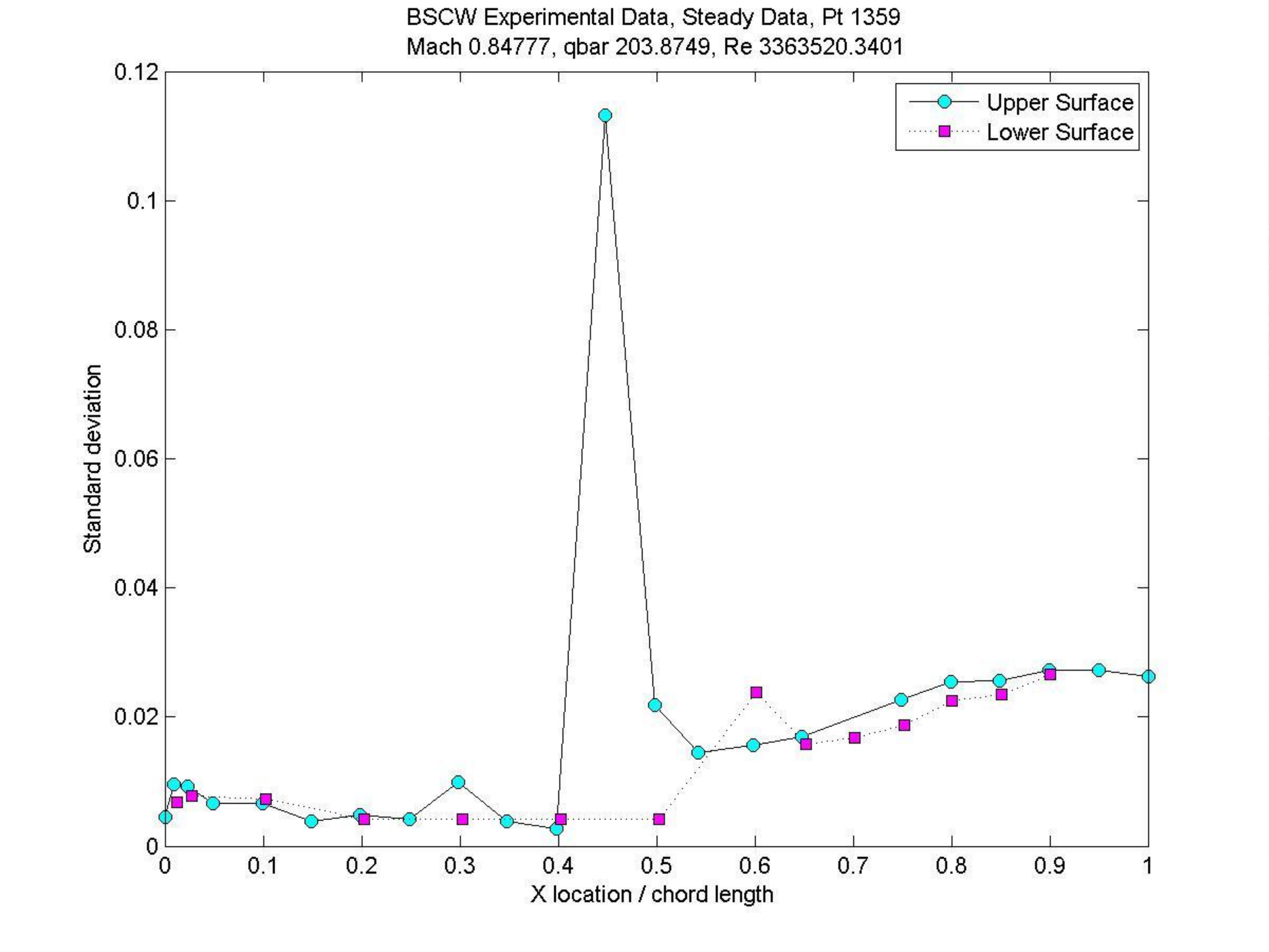

# BSCW Steady Angle

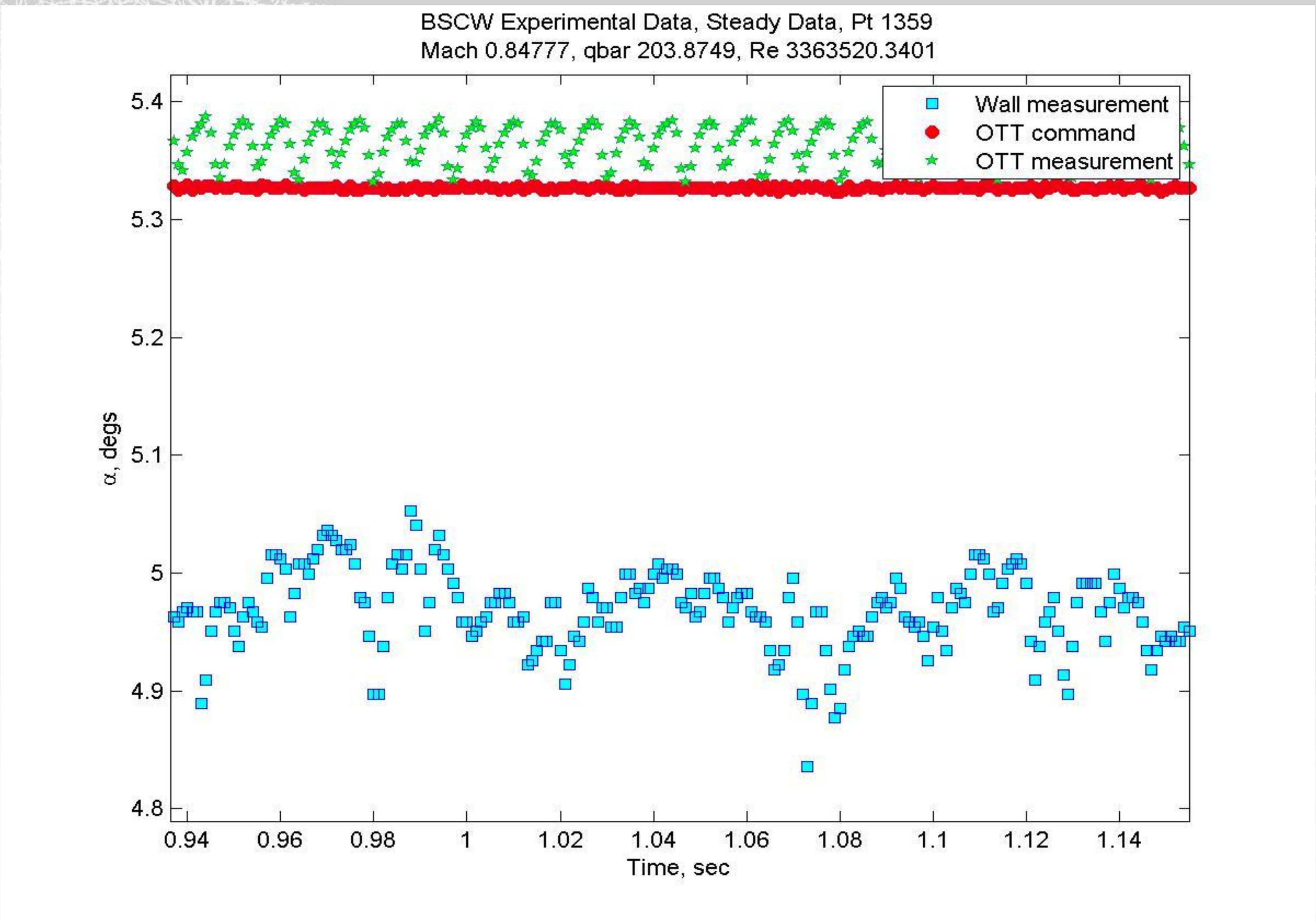

# BSCW non-oscillated data

Splitter plate mode: ~15 Hz
Appears in the Wall Angle Measurement (WALLADT)
Appears in some of the wing sensors

Natural frequencies of BSCW:
24.1 Hz (spanwise 1st bending)
27.0 Hz (in-plane 1st bending)
79.9 Hz (1st torsion)

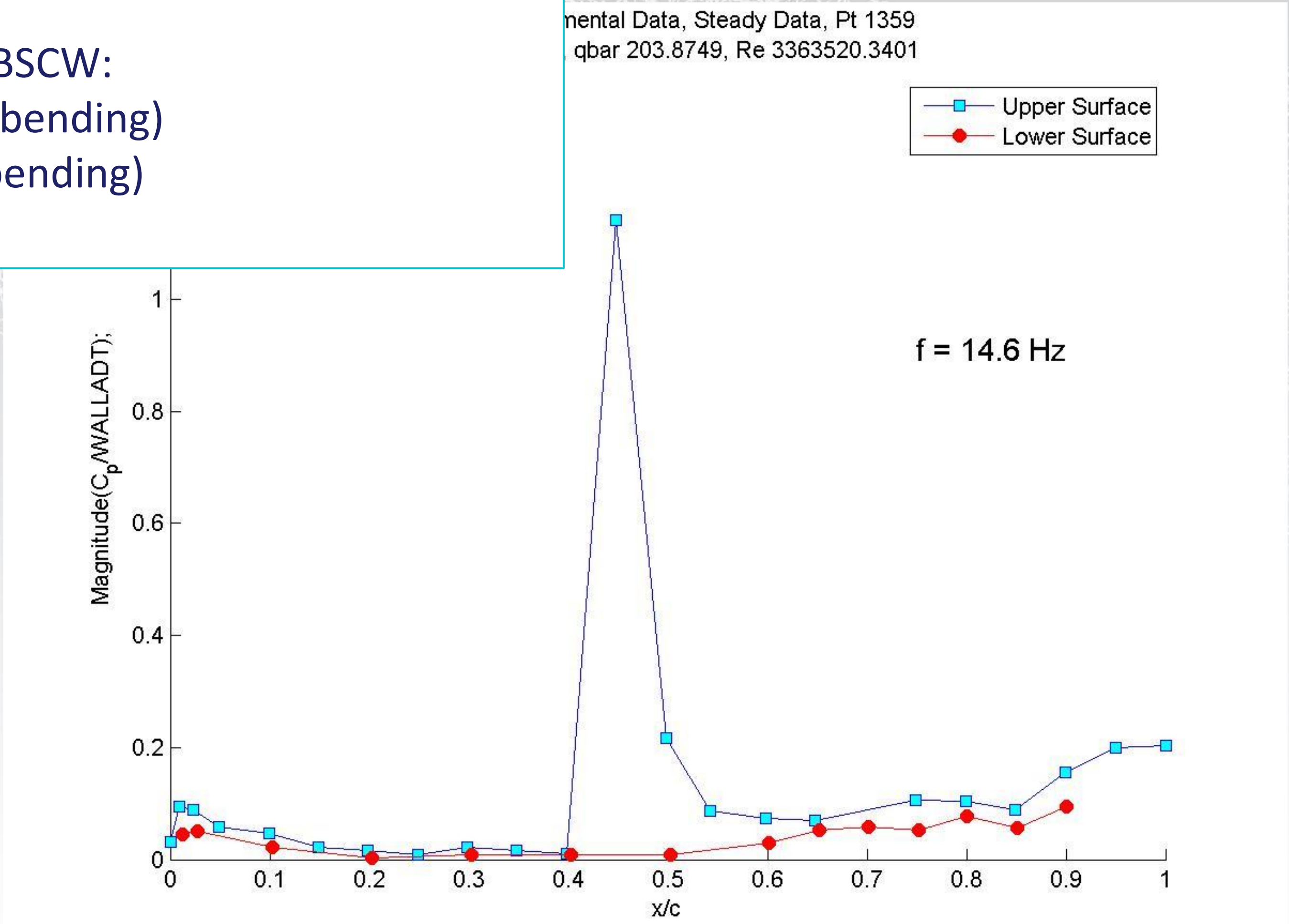

# BSCW Static Data point

Vertical splitter plate mode, 15 Hz

Splitter Plate Accelerometer
in the vertical “Z” direction, SPACCZ

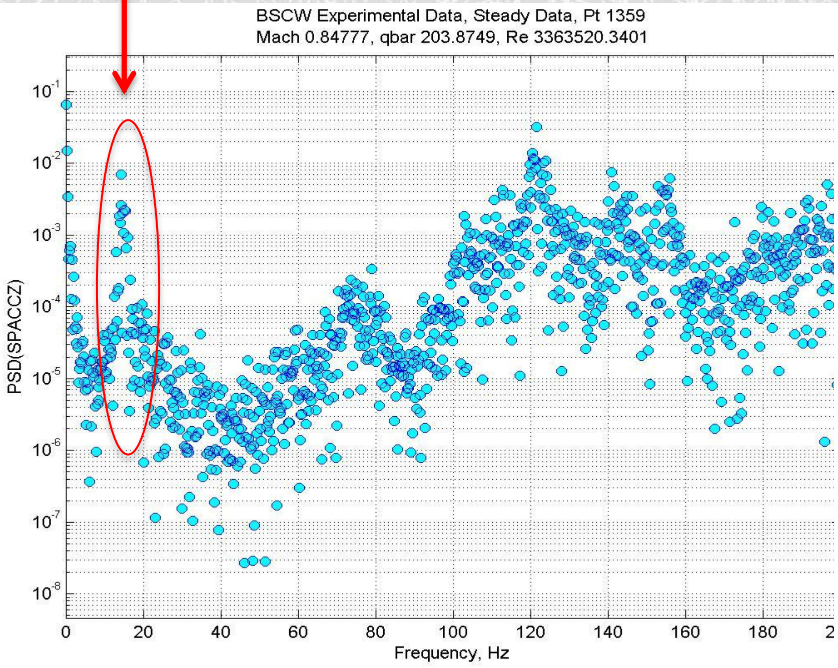


Splitter Plate Accelerometer
in the wall-direction “Y”, SPACCY

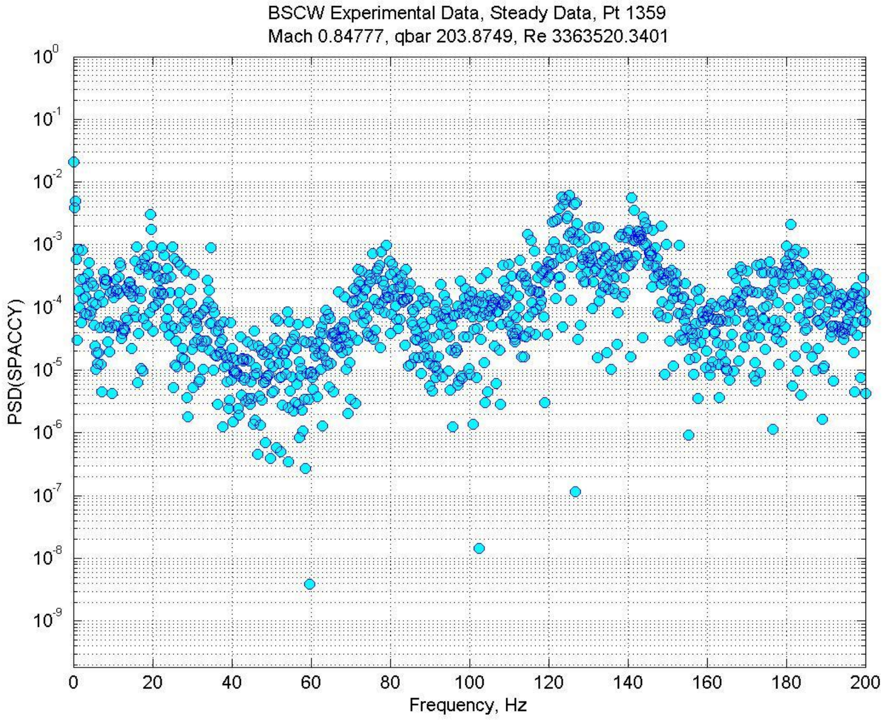

# BSCW Non-oscillated data

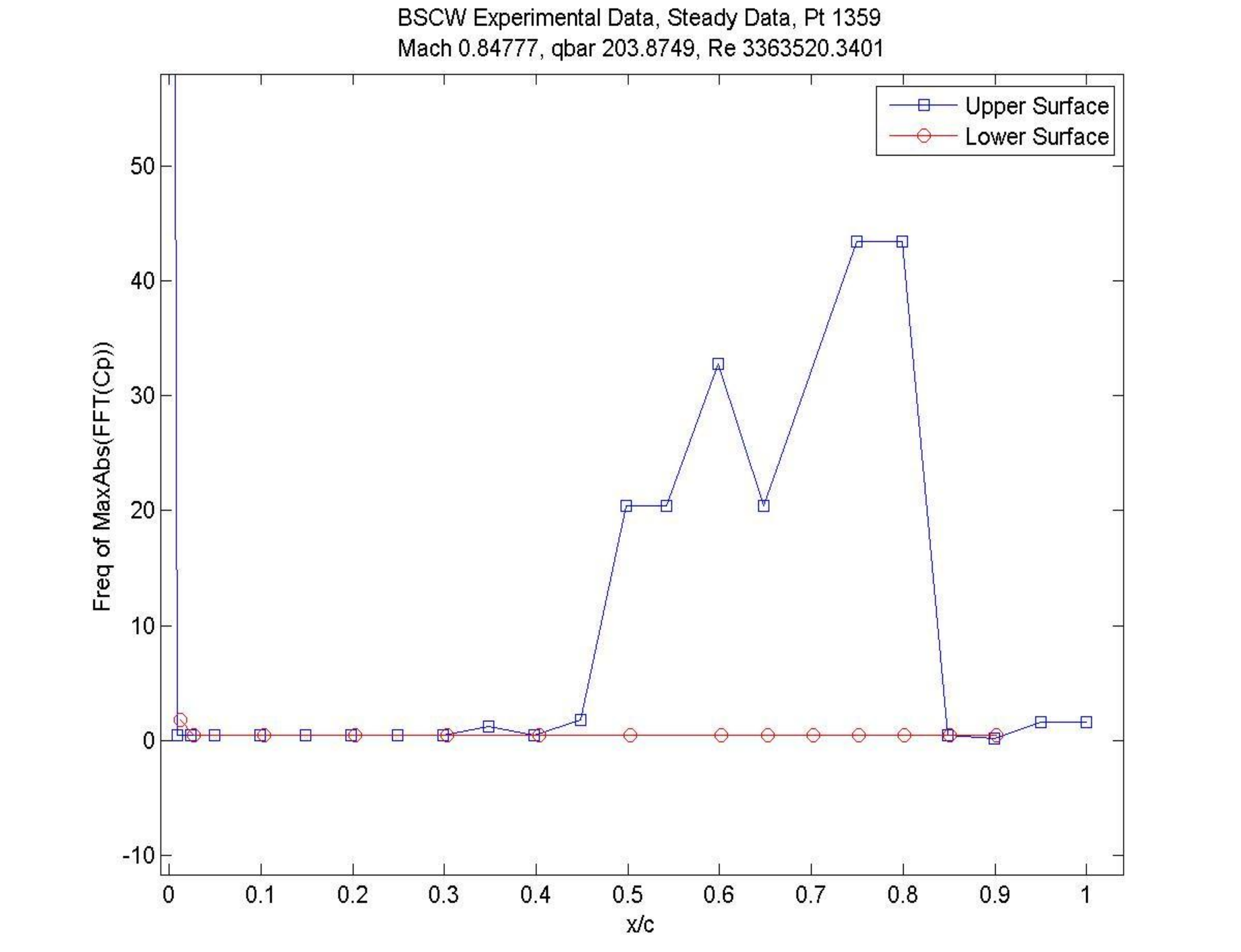


The different upper surface pressure transducers respond most strongly at different frequencies.
?to the different modes of the model?

# BSCW Static point, aeroelastic modes?

Splitter plate mode: ~15 Hz
Appears in the Wall Angle Measurement (WALLADT)
Appears in some of the wing sensors

Natural frequencies of BSCW:
24.1 Hz (spanwise 1st bending)
27.0 Hz (in-plane 1st bending)
79.9 Hz (1st torsion)

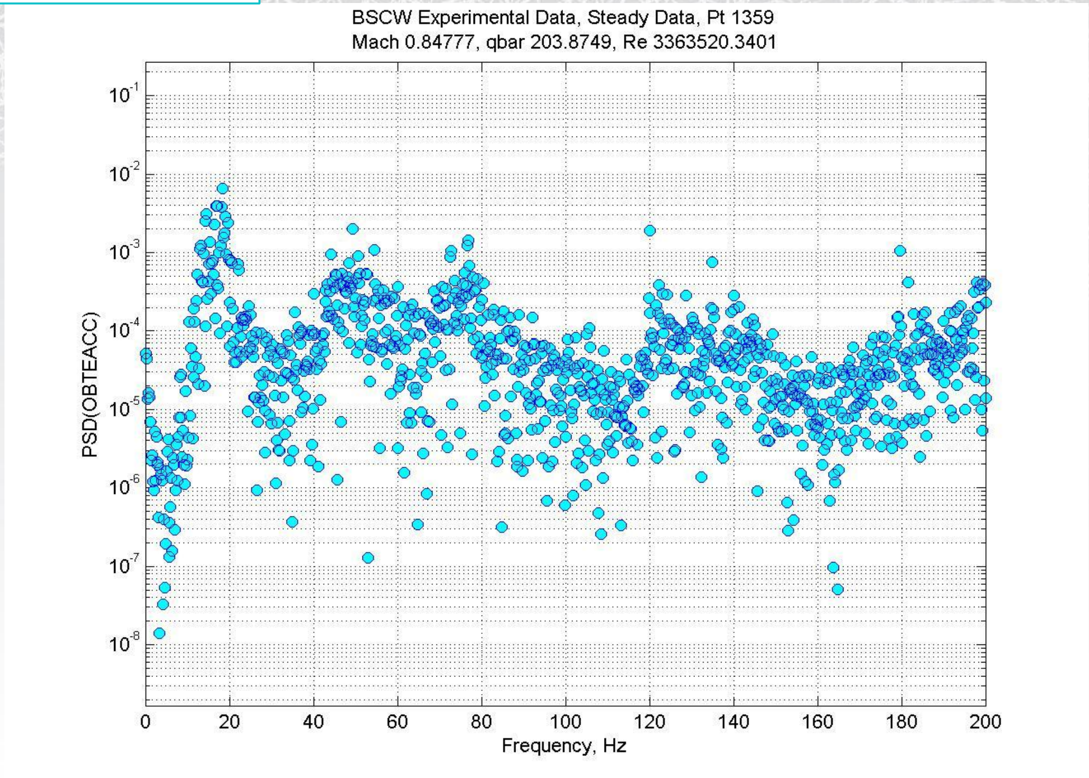

# *BSCW notes*

- Power spectral density functions computed for several sensors. Notice that the WALLADT shows the 15 Hz vertical (gravity-direction) splitter plate mode, but does not show the electronic noise peak at 60 Hz, which is present in the OTTADT.  Notice that, as usual for the BSCW data examined to date, the presumed electronic noise spike at 120 Hz is the dominant peak.
- The 15 Hz splitter plate mode shows up strongly on the SPACCZ , which is the splitter plate accelerometer in the z direction. (tunnel floor to ceiling direction).
- SPACCY has peaks at 20 Hz and near 79 Hz.  Are these the structural modes of the model?  1$^{st}$ spanwise bending mode, air off is at 24 Hz.  1$^{st}$ torsion, air off, is at 80 Hz.
- The PSDs of pressures aren’t shown because nothing really jumps out of them to comment on.

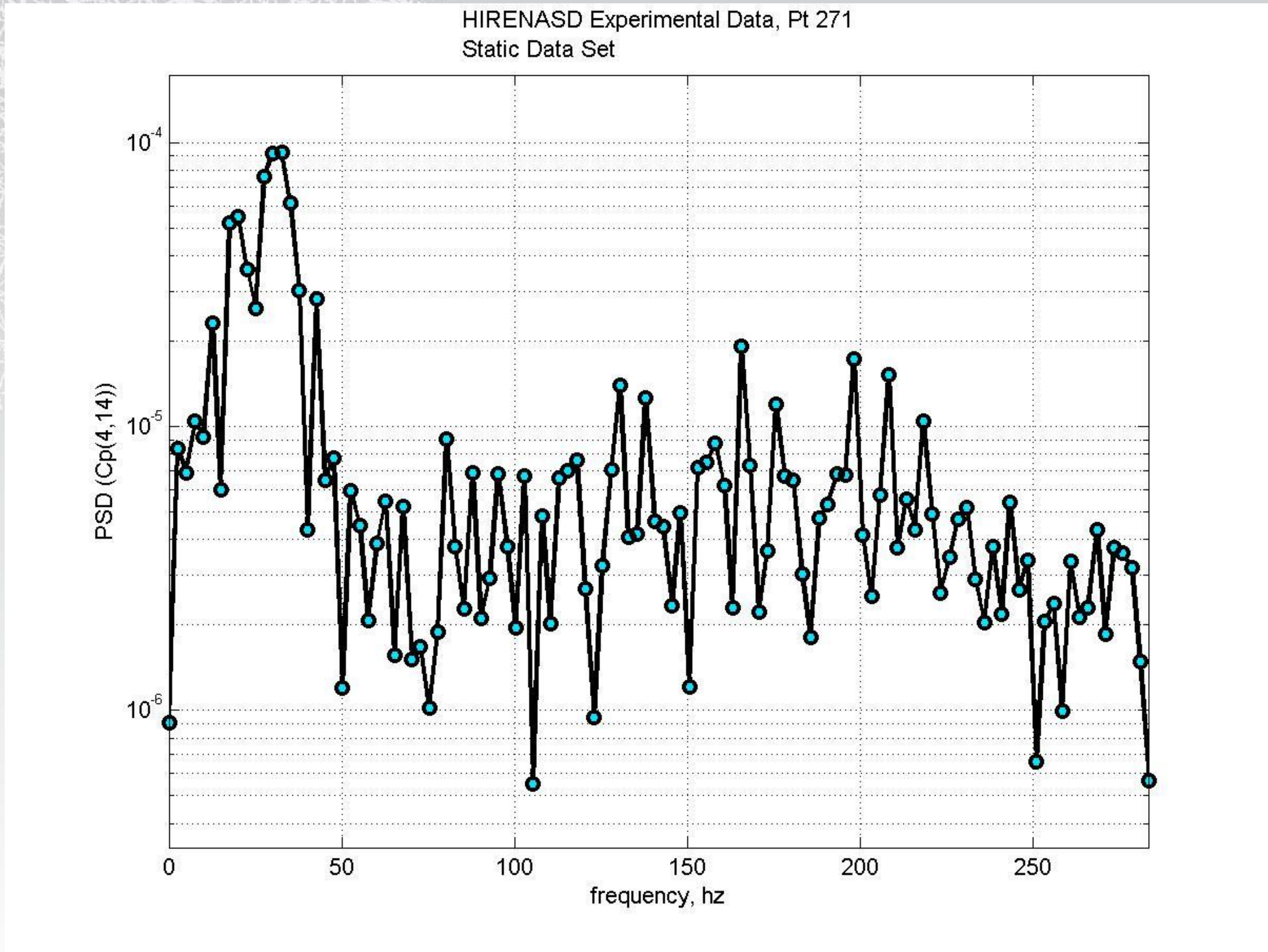
HIRENASD Experimental Data, Pt 271
Static Data Set
PSD (Cp(4,14))
$10^{-4}$
$10^{-5}$
$10^{-6}$
0
50
100
150
200
250
frequency, hz

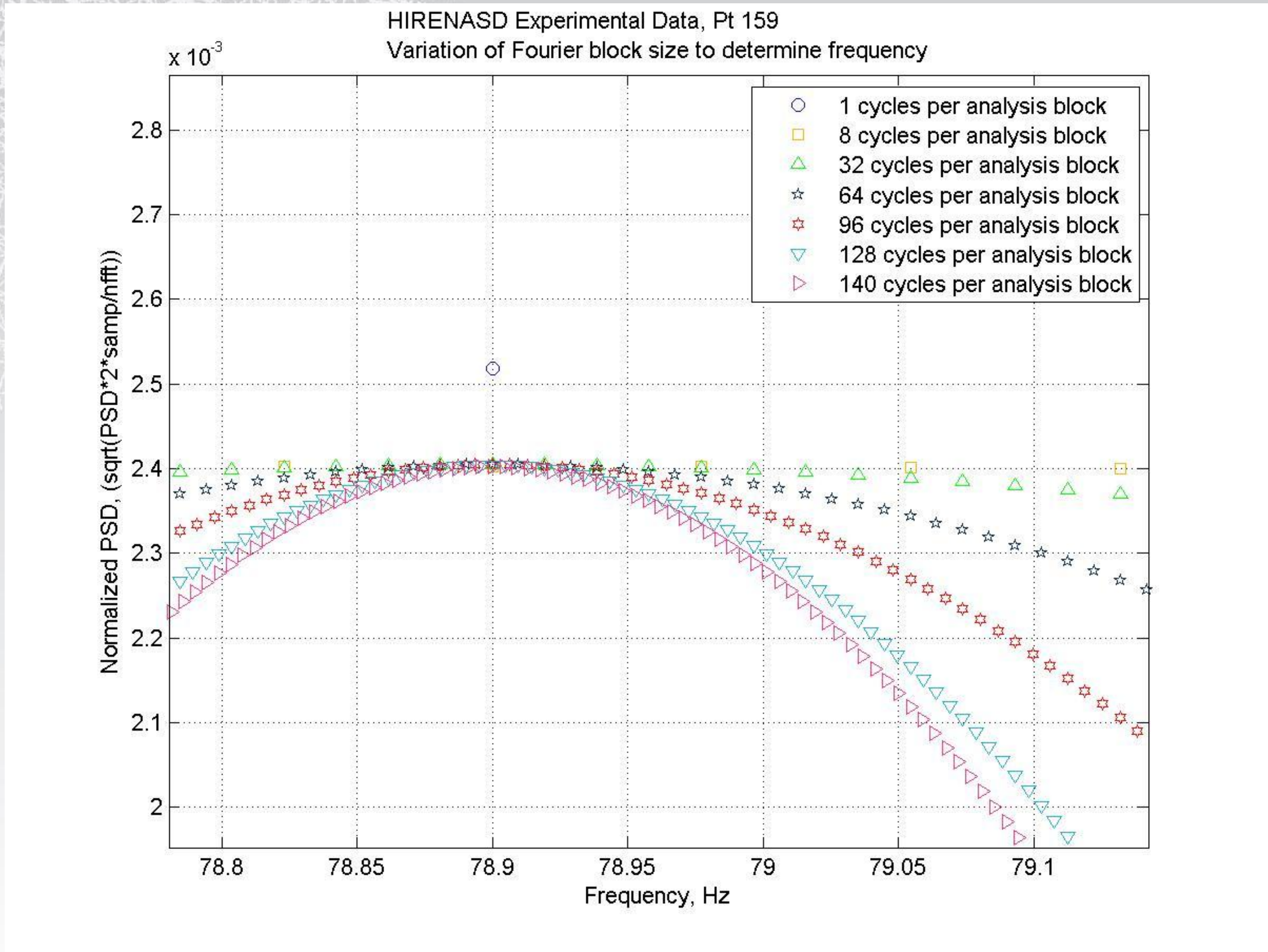

HIRENASD Experimental Data, Pt 159
Variation of Fourier block size to determine frequency
x 10^-3
Normalized PSD, (sqrt(PSD*2*samp/nfft))
Frequency, Hz
1 cycles per analysis block
8 cycles per analysis block
32 cycles per analysis block
64 cycles per analysis block
96 cycles per analysis block
128 cycles per analysis block
140 cycles per analysis block

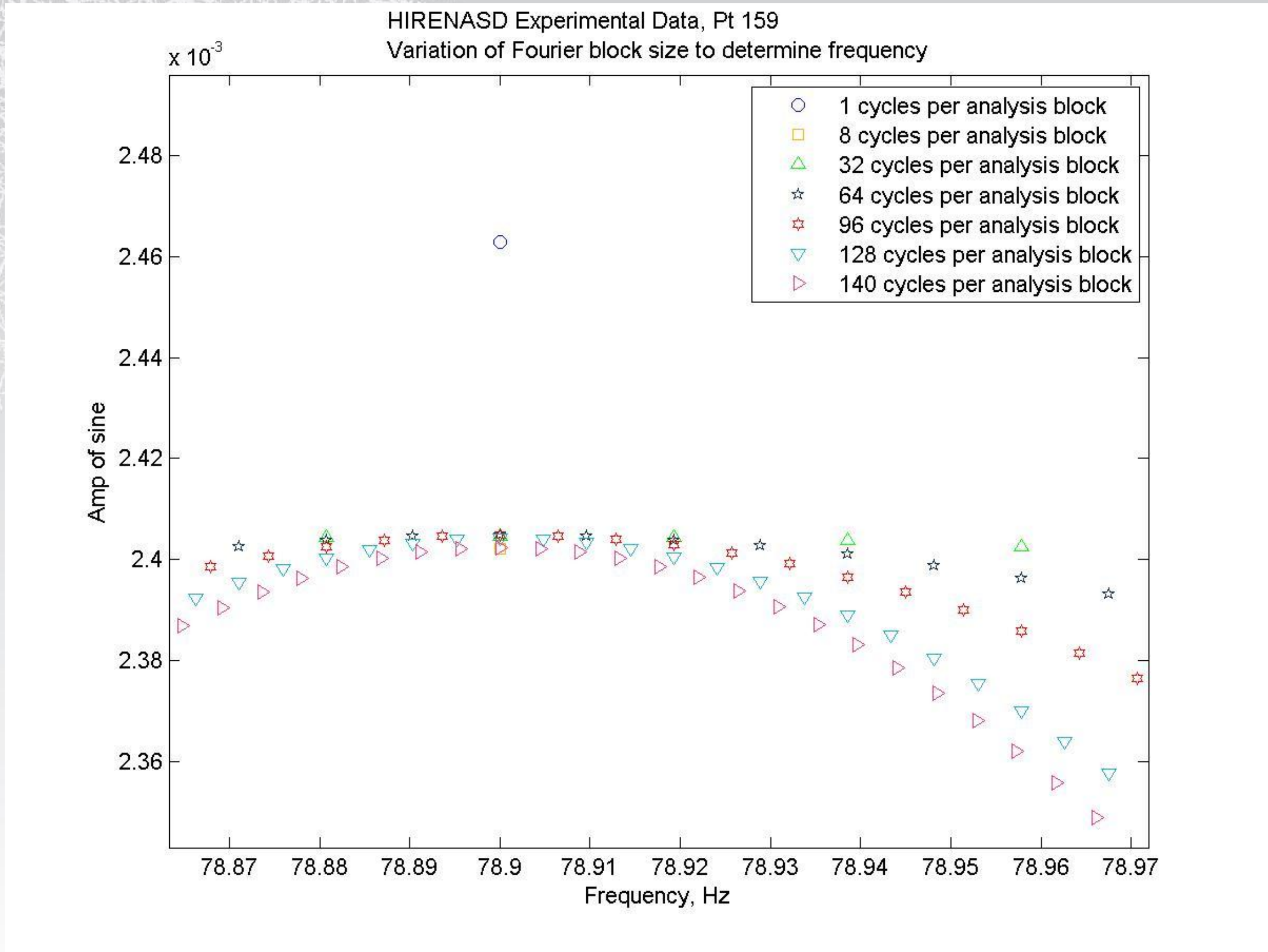
HIRENASD Experimental Data, Pt 159
Variation of Fourier block size to determine frequency
x 10^-3
1 cycles per analysis block
8 cycles per analysis block
32 cycles per analysis block
64 cycles per analysis block
96 cycles per analysis block
128 cycles per analysis block
140 cycles per analysis block
Amp of sine
2.48
2.46
2.44
2.42
2.4
2.38
2.36
78.87
78.88
78.89
78.9
78.91
78.92
78.93
78.94
78.95
78.96
78.97
Frequency, Hz

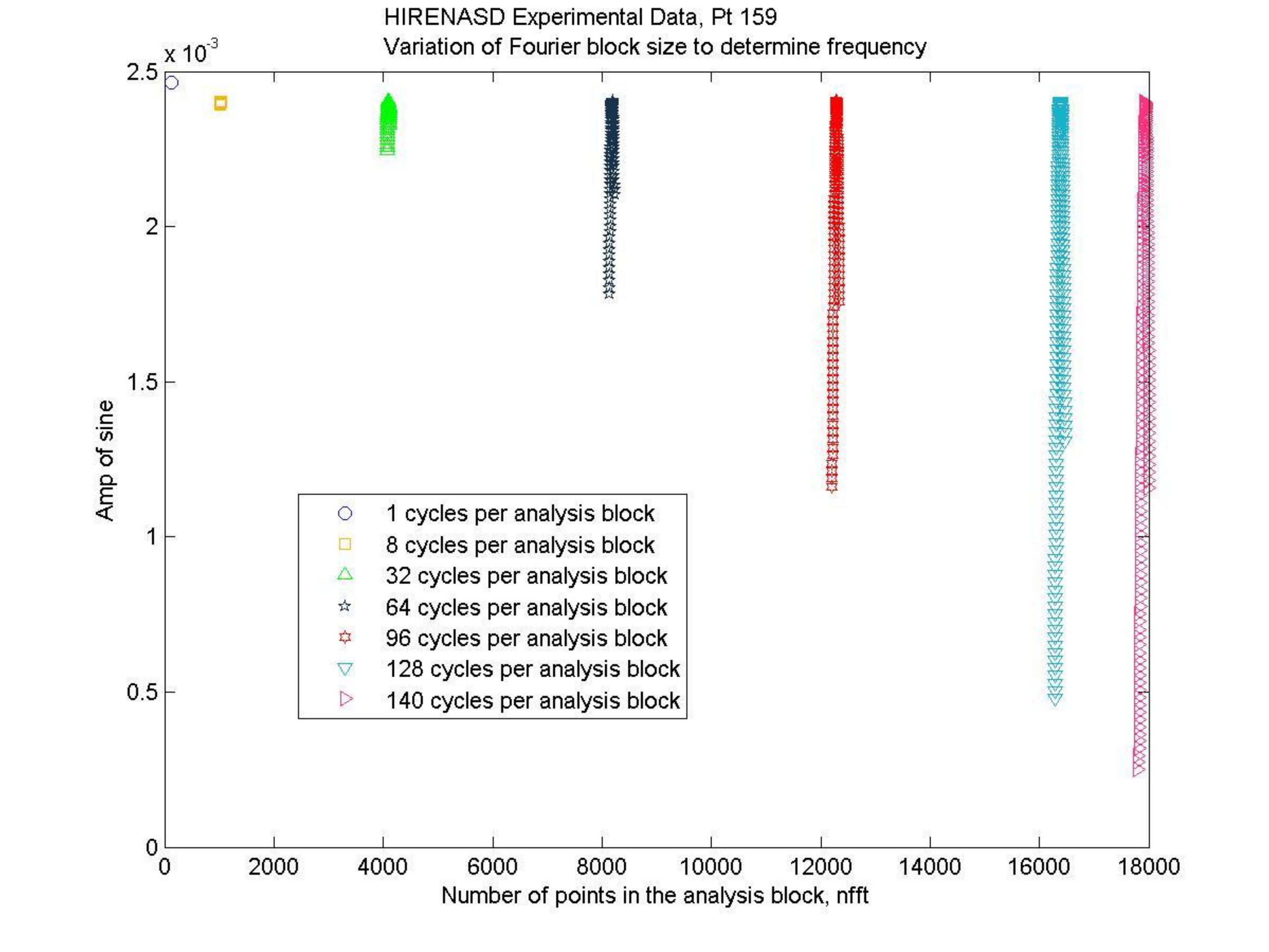

HIRENASD Experimental Data, Pt 159
Variation of Fourier block size to determine frequency
x 10-3
2.5
2
1.5
1
0.5
0
Amp of sine
0
2000
4000
6000
8000
10000
12000
14000
16000
18000
Number of points in the analysis block, nfft
1 cycles per analysis block
8 cycles per analysis block
32 cycles per analysis block
64 cycles per analysis block
96 cycles per analysis block
128 cycles per analysis block
140 cycles per analysis block

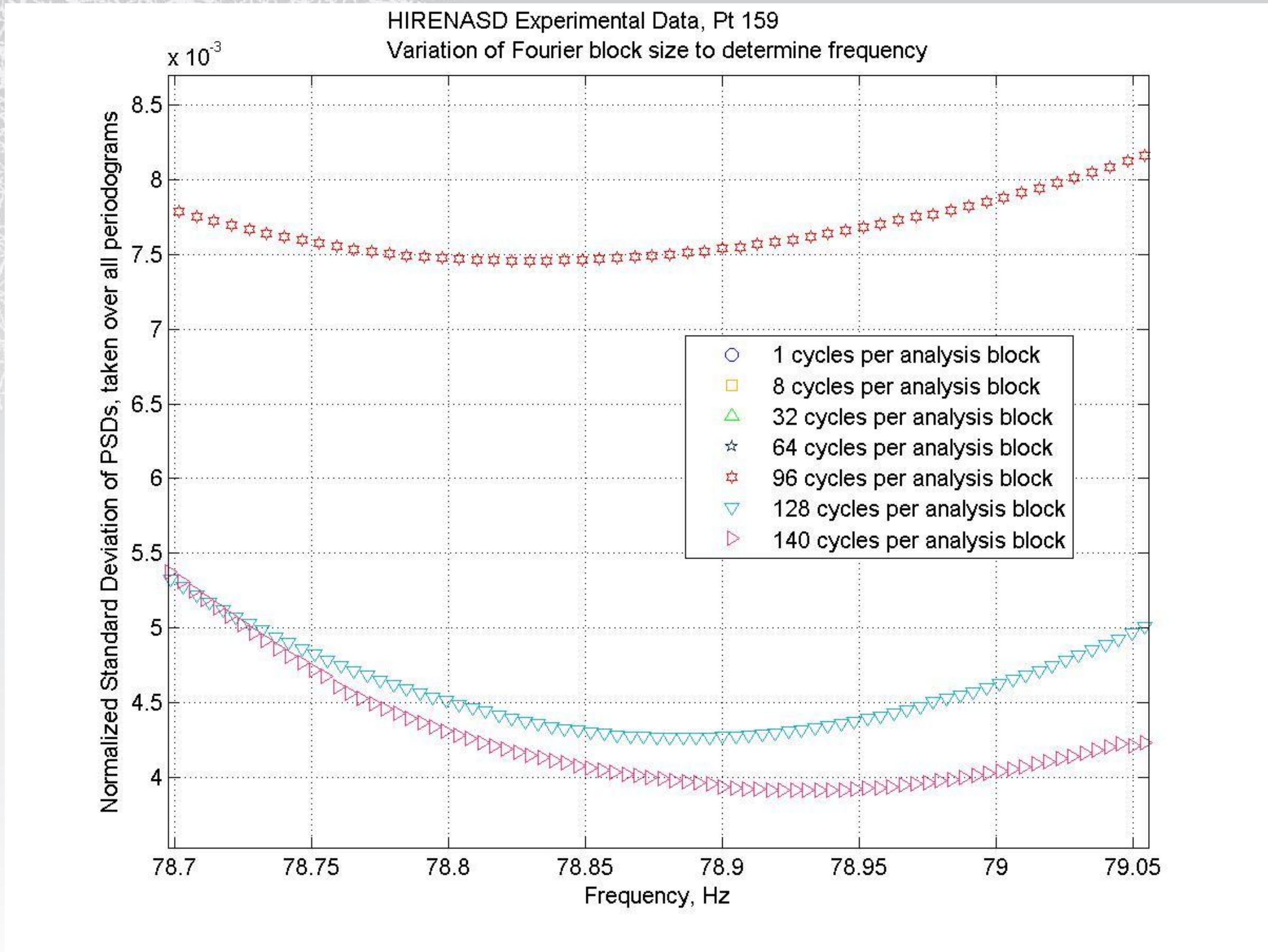
HIRENASD Experimental Data, Pt 159
Variation of Fourier block size to determine frequency
x 10^-3
8.5
8
7.5
7
6.5
6
5.5
5
4.5
4
Normalized Standard Deviation of PSDs, taken over all periodograms
78.7
78.75
78.8
78.85
78.9
78.95
79
79.05
Frequency, Hz
1 cycles per analysis block
8 cycles per analysis block
32 cycles per analysis block
64 cycles per analysis block
96 cycles per analysis block
128 cycles per analysis block
140 cycles per analysis block

# HIRENASD experimental data uncertainty discussion notes

- In computing the transfer functions, the following have been identified as potential sources of variation, error or uncertainty.
- 
- Off frequency (i.e. the excitation is not at exactly the natural or aeroelastic frequency): the variation effect will be highly dependent on damping. Frequency variation or error may be assessable using the stationary point data corresponding to the dynamic test conditions.
- Instrumentation accuracy: requires knowledge of the instrumentation specs and calibrations. This is the easiest source of error or variation to assess because we have instrumentation documentation and calibration documentation. However, in practice, repeat data points have had significantly more variation than could be accounted for through instrumentation accuracy. Jen's note: In the case of Active Aeroelastic Wing test conditions in the Transonic Dynamics Tunnel, the test condition repeat point variation was more than an order of magnitude greater than that indicated by instrumentation accuracy.
  - Pressure transducers
  - Accelerometers
  - SPTs
  - Tunnel measurement systems (static pressure, total pressure, temperature, etc)
- Mean angle of attack error: this can be due to flow redirection or instrumentation error or model alignment
- Model surface effects: If these effects are consistent during a time history, this isn't a cause of variation within the data, just a source of difference from the analytical results which we won't be able to capture or quantify unless we somehow have different model surfaces that allow us to assess this.
- Sidewall effects: as with model surface effects, this isn't a cause of variation within the experimental data set, just a source of difference with respect to the analytical results. Because we don't have an experimental variation on presence of the sidewall, it will be difficult to obtain an error due to the presence of the sidewalls. There was something in one of the AGARD reports regarding accounting for the sidewall, possibly associated with the supercritical wing?
- Tunnel disturbances: Can perhaps be evaluated by examination of two sets of data: one with excitation and one without. Examine the response levels at different frequencies.
- Test condition: variation of the test condition includes H,P,X,T, RPM or calculated parameters like Mach, dynamic pressure. Without experimental data where these were varied, we would have to rely on the analysis to propagate these parameters through and assess the impact on the analytical side.
- Excitation amplitude variation or error
- Data processing effects and assumptions:
  - Non-stationarity: can be assessed by analyzing different subsets of the data
  - Nonlinearity: Can be assessed by detailed examination of the time history and fourier domain data
  - Subsets of the data: see above
  - Method of reduction
  - Fourier processing parameters
    - Fourier block size
    - Overlap
    - Window
- 
- Data acquisition effects:
  - Voltage disturbances due to:
    - Cable lengths
    - Analog to digital converters
- 

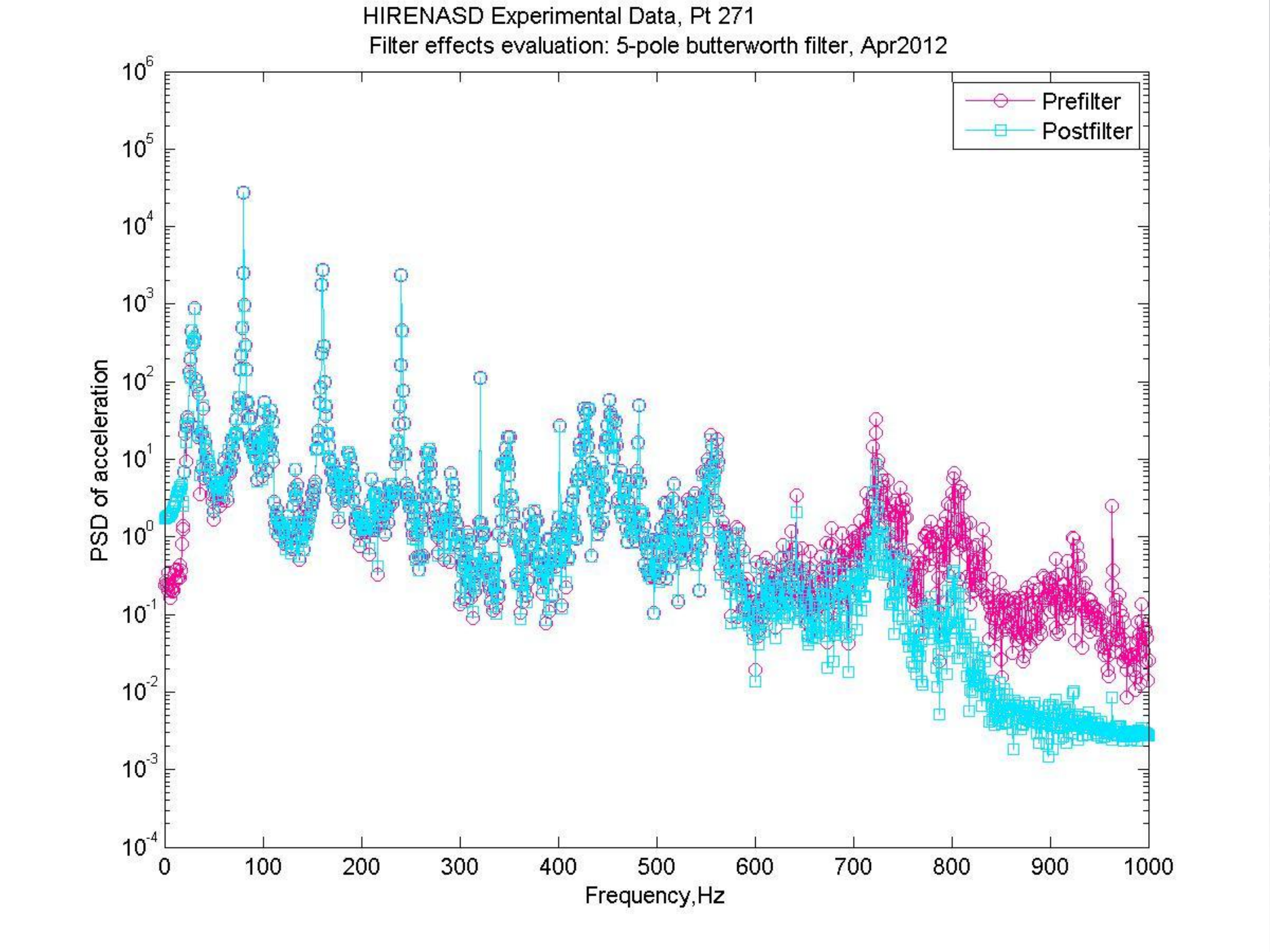

HIRENASD Experimental Data, Pt 271
Filter effects evaluation: 5-pole butterworth filter, Apr2012
Prefilter
Postfilter
PSD of acceleration
Frequency,Hz
$10^{6}$
$10^{5}$
$10^{4}$
$10^{3}$
$10^{2}$
$10^{1}$
$10^{0}$
$10^{-1}$
$10^{-2}$
$10^{-3}$
$10^{-4}$
0
100
200
300
400
500
600
700
800
900
1000

# PSD of pressure

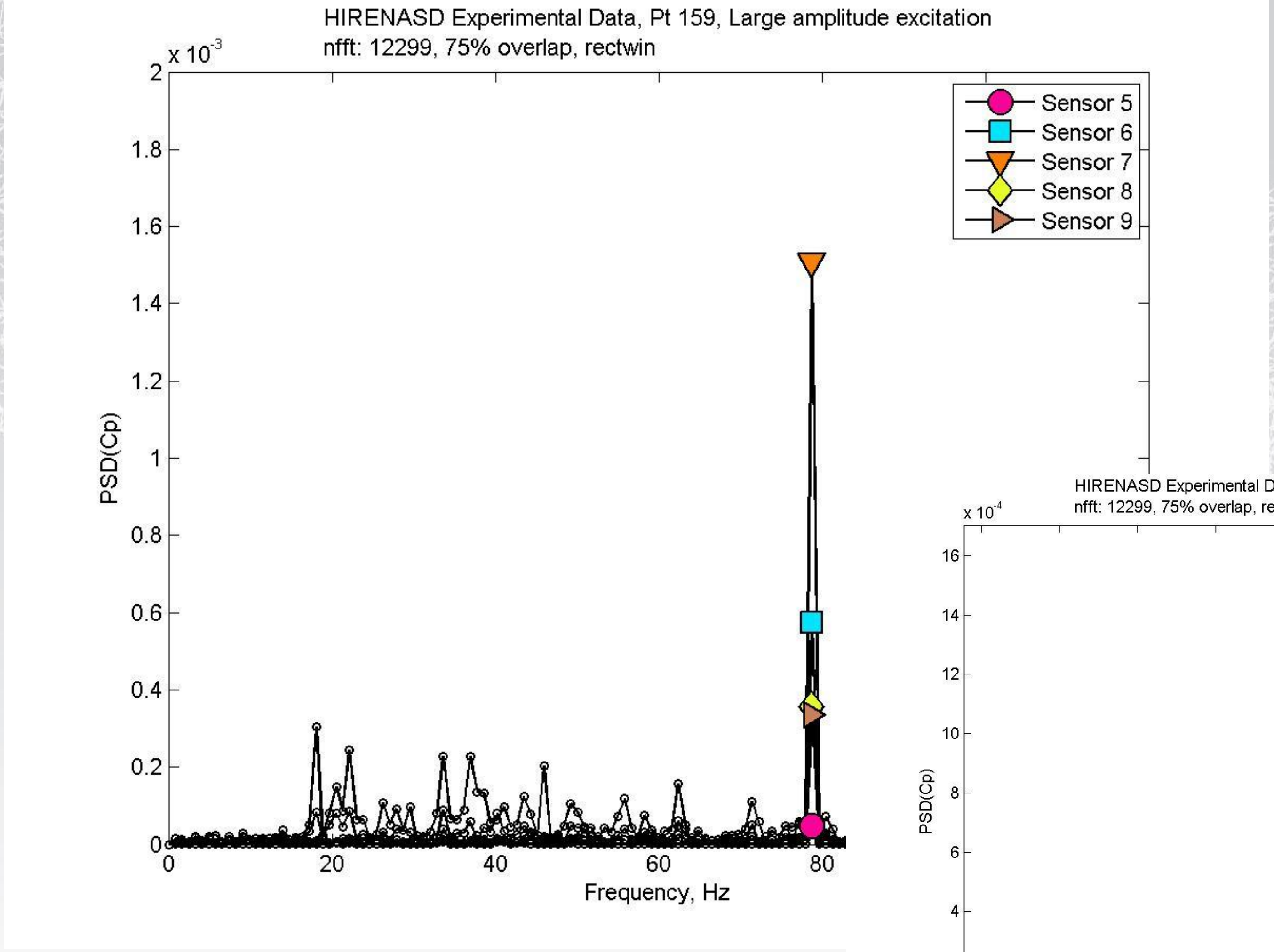


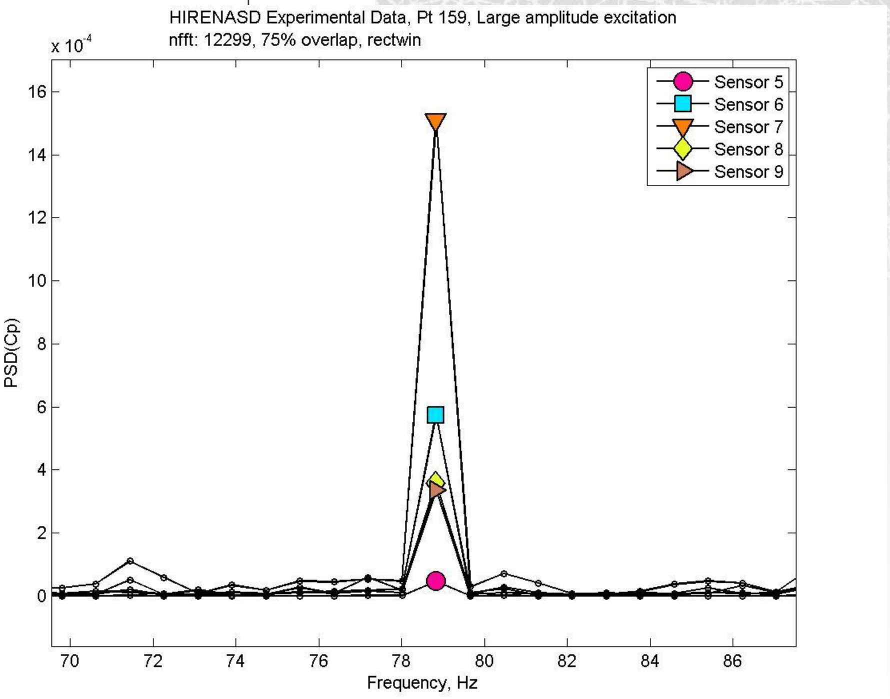

# HIRENASD unsteady time history data: upper surface pressures